INFLUENCES OF INTERPLANETARY MAGNETIC FIELD ON THE VARIABILITY OF THE AEROSPACE MEDIA

A THESIS SUBMITTED TO
THE GRADUATE SCHOOL OF NATURAL AND APPLIED SCIENCES
OF
MIDDLE EAST TECHNICAL UNIVERSITY

BY

TOLGA YAPICI

IN PARTIAL FULFILLMENT OF THE REQUIREMENTS
FOR
THE DEGREE OF MASTER OF SCIENCE
IN
AEROSPACE ENGINEERING

SEPTEMBER 2007

Approval of the thesis

INFLUENCES OF INTERPLANETARY MAGNETIC FIELD ON THE VARIABILITY OF THE AEROSPACE MEDIA

submitted by **TOLGA YAPICI** in partial fulfillment of the requirements for the degree of **Master of Science in Aerospace Engineering Department, Middle East Technical University** by,

Prof. Dr. Canan Özgen
Dean, Gradute School of **Natural and Applied Sciences** _____

Prof. Dr. İsmail Hakkı Tuncer
Head of Department, **Aerospace Engineering** _____

Prof. Dr. Yurdanur Tulunay
Supervisor, **Aerospace Engineering Dept., METU** _____

Examining Committee Members:

Assoc. Prof. Dr. Serkan Özgen
Aerospace Engineering Dept., METU _____

Prof. Dr. Yurdanur Tulunay
Aerospace Engineering Dept., METU _____

Assoc. Prof. Dr. Altan Kayran
Aerospace Engineering Dept., METU _____

Assoc. Prof. Dr. Tolga Çiloğlu
Electrical and Electronical Engineering Dept., METU _____

Dr. Sartuk Karasoy
ROKETSAN _____

Date: _____

I hereby declare that all information in this document has been obtained and presented in accordance with academic rules and ethical conduct. I also declare that, as required by these rules and conduct, I have fully cited and referenced all material and results that are not original to this work.

Name, Last Name: TOLGA YAPICI

Signature :

ABSTRACT

INFLUENCES OF INTERPLANETARY MAGNETIC FIELD ON THE VARIABILITY OF THE AEROSPACE MEDIA

Yapıcı, Tolga

M.S., Department of Aerospace Engineering

Supervisor : Prof. Dr. Yurdanur Tulunay

September 2007, 50 pages

The Interplanetary Magnetic Field (IMF) has a controlling effect on the Magnetosphere and Ionosphere. The objective in this work is to investigate the probable effects of IMF on Ionospheric and Geomagnetic response. To fulfill the objective the concept of an event has been created based on the polarity reversals and rate of change of the interplanetary magnetic field components, B_z and B_y. Superposed Epoch Method (SPE) was employed with the three event definitions, which are based on IMF B_z southward turnings ranging from 6 to 11 nT in order to quantify the effects of IMF B_y and B_z. For the first event only IMF B_z turnings were taken into account while for the remaining, positive and negative polarity for IMF B_y were added. Results showed that the increase in the magnitude of IMF B_z turnings increased the drop of F layer critical frequency, f_0F2. The drop was almost linear with the increase in magnitude of polarity reversals. Reversals with a positive IMF B_y has resulted in the continuation of geomagnetic activity more than 4 days, that is to say, the energy, that has penetrated as a consequence of reversal with a positive B_y polarity, was stored in outer Magnetosphere,whereas, with a negative IMF B_y the energy was consumed in a small time scale.

At the second step of the work, although conclusions about geomagnetic activity could be done, as a consequence of data gaps for f_0F2 in addition to having low numbers of events,

characterization of f_0F2 due to constant IMF B_y polarity could not be accomplished. Thus, a modeling attempt for the characterization of the response due to polarity reversals of IMF components with the Genetic Programming was carried out. Four models were constructed for different polarity reversal cases and they were used as the components of one general unique model. The model is designed in such a way that given 3 consecutive value of f_0F2, IMF B_y and IMF B_z, the model can forecast one hour ahead value of f_0F2. The overall model, GETY-IYON was successful at a normalized error of 7.3%.

Keywords: Magnetosphere, Ionosphere, Interplanetary Magnetic Field, Modeling, Genetic Programming

ÖZ

GEZEGENLERARASI MANYETIK ALANININ HAVACILIK VE UZAY ORTAMINDAKI OLASI ETKILERI

Yapıcı, Tolga
Yüksek Lisans, Havacılık ve Uzay Mühendisligi Bölümü
Tez Yöneticisi : Prof. Dr. Yurdanur Tulunay

Eylül 2007, 50 sayfa

Gezegenlerarası Manyetik Alanın (IMF), Manyetosfer ve İyonküre üzerinde kontrol edici etkisi vardır. Bu çalışmada amaç Gezegenlerarası Manyetik Alanın İyon küresel ve Jeomanyetik olası tepkileri incelenmektedir. IMF'nin z yönündeki bileşeni, IMF B_z'nin 6 nT ile 11 nT arasında değişen büyüklüklerinde, 3 adet "olay" tanımına dayalı "Superposed Epoch" yöntemi uygulanmıştır. Birinci "olay" tanımı için sadece IMF B_z kutuplaşma dönüşleri değerlendirilirken, diğerleri için positif ve negatif IMF B_y kutuplaşması eklenmiştir. Sonuçlar, IMF B_z kutuplaşma dönüşlerindeki büyüklüğün artışının, F katmanı kritik frekansı, f_0F2'daki düşüşü artırdığı göstermiştir. Düşüş, neredeyse, kutuplaşma dönüşünün büyüklüğü ile doğrusal olarak değişmektedir. Positif IMF B_y ve IMF B_z kutuplaşma dönüşleri sırasında, Jeomanyetik aktivitenin 4 günden fazla devam ettiği sonucuna varılmıştır.

Çalışmanın ikinci basamağında, Jeomanyetik aktivite hakkında bazı sonuçlara varılabilmişse de, düşük sayıdaki olaylara ek olarak f_0F2 verilerindeki boşluklardan ötürü, f_0F2'ye sabit IMF B_y kutuplaşmasının etkisinin tanımlanması yapılamamıştır. Bu yüzden, IMF kutuplaşma dönüşlerinin etkilerinin tanımlanmasıiçin "Genetik Programlama"yla modelleme denemesi yapılmıştır. Değişik kutuplaşma dönüşleri için dört model oluşturulmuş ve bu modeller tek genel ve eşsiz bir modelin bileşenleri olarak kullanılmıştır. Model verilen ardışık 3 saat-

lik f_0F2, IMF B_y ve IMF B_z verileriyle bir saat sonraki f_0F2 değerini kestirmek için dizayn edilmiştir.

Anahtar Kelimeler: Manyetik Küre, İyonküre, Gezegenler Arası Manyetik Alan, Modelleme, Genetik Programlama

To my family and my lovely girl friend

ACKNOWLEDGMENTS

I would like to express my gratitude to my advisor Prof. Dr. Yurdanur Tulunay and Prof. Dr. Ersin Tulunay for her help, advice and guidance during my thesis.

There are no words to describe the appreciation and gratitude I feel for my family. I am proud to have such a family which gave me valuable advice and support when I needed it most. And special thanks to my lovely girlfriend for her endless love, faith in me, understanding and continued patience. Also, I would like to thank my colleagues and my friends, Emre Altuntaş and Zeynep Kocabaş for their help during the whole study.

TABLE OF CONTENTS

ABSTRACT iv

ÖZ vi

DEDICATON viii

ACKNOWLEDGMENTS ix

TABLE OF CONTENTS x

LIST OF TABLES xiii

LIST OF FIGURES xiv

CHAPTERS

1 INTRODUCTION 1

1.1 Solar Wind and Interplanetary Magnetic Field 2

1.2 Magnetosphere 2

1.3 Ionosphere 2

1.4 Interaction of Magnetosphere and Ionosphere 5

1.5 Literature Survey 5

1.6 Summary 6

2 DATA 8

2.1 Data Used 8

2.1.1 Interplanetary Magnetic Field 8

2.1.2 Geomagnetic Indices 9

2.1.2.1 Kp 10

2.1.2.2 Dst 11

2.1.3 F layer Critical Frequency, f_0F2 12

2.2 Data Organization 12

3 SUPERPOSED EPOCH APPROACH 13
3.1 Method of Analysis 13
3.1.1 SPE Analysis of f_0F2 Values 13
3.2 Results 15
3.2.1 Superposed Epoch Analysis Results for IMF B_z reversals . 19
3.2.1.1 Effects on Geomagnetic Activity 19
Effects on Kp 19
Effects on Dst 20
3.2.1.2 Effects on F layer Critical Frequency, f_0F2 . . 21
3.2.2 Superposed Epoch Analysis Results for IMF B_z reversals during Steady IMF B_y Polarity 22
3.2.2.1 Effects on Geomagnetic Activity 22
Effects on Kp 22
Effects on Dst 24
3.2.2.2 Effects on F layer Critical Frequency, f_0F2 . . 24
4 GENETIC PROGRAMMING APPROACH 27
4.1 Method of Analysis 27
4.1.1 Operators 29
4.1.2 Function Sets 31
4.1.3 Creating Initial Generation 31
4.1.4 Creating Initial Individuals 31
4.1.5 Generations and Error Analysis 32
4.1.6 Genetic Programming for f_0F2 Values, GETY-IYON . . . 32
4.1.6.1 Construction of Models 32
4.2 Results 34
5 DISCUSSION and CONCLUSION 45
REFERENCES 46
APPENDICES
A Coordinate Systems 48
A.1 The Geocentric Solar Ecliptic System 48

A.2 Geocentric Solar Magnetospheric System 48
B Relevant Publications and Activities 49

LIST OF TABLES

TABLES

Table 3.1 Number of Occurances of Events (1973-1993) 14

Table 4.1 Relative Errors of 5 seperate GETY models 35

LIST OF FIGURES

FIGURES

Figure 1.1 The Structure of the Magnetosphere 3

Figure 2.1 IMF Variation during January, 1973 9

Figure 2.2 3-h planetary Kp index variation during January, 1973 10

Figure 2.3 Disturbance Storm Time (Dst) index variation during January, 1973 11

Figure 3.1 Diurnal Variation of δf_0F2 for Arkhangelsk Vertical Ionosonde 16

Figure 3.2 Probabilities and Cumulative Probabilities of IMF B_z 16

Figure 3.3 Probabilities and Cumulative Probabilities of f_0F2 values 17

Figure 3.4 Probabilities and Cumulative Probabilities of Dst index 17

Figure 3.5 Probabilities and Cumulative Probabilities of Kp index 18

Figure 3.6 SPE Results of Kp index for southward turnings with $\delta B_z \geq 6$ nT/h and ≥ 11 nT/h 19

Figure 3.7 SPE Results of Dst index for southward turnings with $\delta B_z \geq 6$ nT/h and ≥ 11 nT/h 20

Figure 3.8 SPE Results for southward turnings with $\delta B_z \geq 6$nT/h and 11nT/h for Arkhangelsk 21

Figure 3.9 SPE Results for southward turnings with $\delta B_z \geq 6$nT/h and 11nT/h for Slough 22

Figure 3.10 SPE Results of Kp index for southward turnings with $\delta B_z \geq 6$nT/h for three IMF B_y criteria 23

Figure 3.11 SPE Results of Kp index for southward turnings with $\delta B_z \geq 11$nT/h for three IMF B_y criteria 23

Figure 3.12 SPE Results of Dst index for southward turnings with $\delta B_z \geq 6$nT/h for three IMF B_y criteria 24

Figure 3.13 SPE Results of Dst index for southward turnings with $\delta B_z \geq 11$nT/h for three IMF B_y criteria 25

Figure 3.14 SPE Results of f_0F2 for southward turnings with $\delta B_z \geq 6$nT/h for three IMF B_y criteria 26

Figure 4.1 A sample tree structure of an individual 28

Figure 4.2 Deoxyribonucleic Acid (DNA) 28

Figure 4.3 The crossing-over process for human DNA 30

Figure 4.4 A sample crossing over operation 30

Figure 4.5 Structure of the GETY-IYON 34

Figure 4.6 Observed Values (in red) and Genetic Programming Results (in blue) of f_0F2 values and the variation of Sun Spot Number 35

Figure 4.7 Observed Values (in red) and Genetic Programming Results (in blue) of f_0F2 values for the year 1982 36

Figure 4.8 Observed Values (in red) and Genetic Programming Results (in blue) of f_0F2 values for the year 1987 36

Figure 4.9 Observed Values (in red) and Genetic Programming Results (in blue) of f_0F2 values for the year 1982 around Spring (Vernal) Equinox 37

Figure 4.10 Observed Values (in red) and Genetic Programming Results (in blue) of f_0F2 values for March 1982 (around Spring Equinox) 37

Figure 4.11 Observed Values (in red) and Genetic Programming Results (in blue) of f_0F2 values for the year 1987 around Spring (Vernal) Equinox 38

Figure 4.12 Observed Values (in red) and Genetic Programming Results (in blue) of f_0F2 values for March 1987 (around Spring Equinox) 38

Figure 4.13 Observed Values (in red) and Genetic Programming Results (in blue) of f_0F2 values for the year 1982 around Summer Solstice 39

Figure 4.14 Observed Values (in red) and Genetic Programming Results (in blue) of f_0F2 values for June 1982 (around Summer Solstice) 40

Figure 4.15 Observed Values (in red) and Genetic Programming Results (in blue) of f_0F2 values for the year 1987 around Summer Solstice 40

Figure 4.16 Observed Values (in red) and Genetic Programming Results (in blue) of f_0F2 values for June 1987 (around Summer Solstice) 41

Figure 4.17 Observed Values (in red) and Genetic Programming Results (in blue) of f_0F2 values for the year 1982 around Fall (Autumnal) Equinox 41

Figure 4.18 Observed Values (in red) and Genetic Programming Results (in blue) of f_0F2 values for September 1982 (around Fall (Autumnal) Equinox) 42

Figure 4.19 Observed Values (in red) and Genetic Programming Results (in blue) of f_0F2 values for the year 1987 around Fall (Autumnal) Equinox 42

Figure 4.20 Observed Values (in red) and Genetic Programming Results (in blue) of f_0F2 values for September 1987 (around Fall (Autumnal) Equinox) 43

Figure 4.21 Observed Values (in red) and Genetic Programming Results (in blue) of f_0F2 values for December 1982 (around Winter Solstice) 43

Figure 4.22 Observed Values (in red) and Genetic Programming Results (in blue) of f_0F2 values for December 1987 (around Winter Solstice) 44

CHAPTER 1

INTRODUCTION

The dependence of society to technology increased in recent years as the technology has enhanced. Moreover, in addition to technology, the dependence of society to nature also increased.

Today's space technology is based on electrical and electronical circuits which is vulnerable to sudden changes in temperature, pressure, radiation, etc. Thus, the Space Weather, which can be defined as the collective, often violent, changes in the space environment surrounding Earth, plays an important role on space-based assets for navigation, communication, military reconnaissance and exploration[7]. Space Weather effects on technology can be experienced both in deep space and on the surface of the Earth. Some of the effects are surface charging, internal charging, displacement damage, single event effects (single event upsets and single event latchups) and radiation dose.

Today's challenge is to learn quantitatively predicting and forecasting the state of the magnetosphere and ionosphere from measured solar wind and interplanetary magnetic field conditions. Engineering and life sciences are needed to evaluate the hazards and risks on the technology and mankind[1]. In this work, telecommunication point of view for the effect of Space Weather was investigated with two methods of analysis. First method was employed for the characterization of the effect and the other method was employed for the construction of model for forecasting effects of some specific cases.

1.1 Solar Wind and Interplanetary Magnetic Field

The Sun is the source of most of Space Weather effects. The Sun's outer most layer, Corona, does not have a rigid boundary, instead it has a ragged structure blending into the background[9]. The extension of the Solar Corona to large distances is named as "Solar Wind"[14]. The effects of the Sun are carried with a continuously streaming Solar Wind to the Earth. The high conductivity of the Solar Wind traps the magnetic field in itself, then the supersonic flowing frozen-in magnetic field of Solar Wind forms the Interplanetary Magnetic Field, which is crucial for the formation and the variability of the Magnetosphere.

1.2 Magnetosphere

Solar Wind which is a moving conducting surface is not allowed by Earth's internal magnetic field to penetrate, thus, in order to oppose the Earth's internal magnetic field, a current system is generated on the boundary. On the sunward boundary, some of the magnetic field lines are broken and pushed away from the Sun [14]. Since the Maxwell's Equation, $\nabla \cdot \vec{B} = 0$, where $\vec{B}$ is the magnetic field vector, states that there cannot be any monopoles, it can be said that these pushed back magnetic field lines connect to their conjugates at a point that can be imagined as infinity. Figure 1.1 shows the structure of the Magnetosphere.

During disturbed conditions (i.e. Magnetospheric Storms and Substorms), most of the time, the z component of IMF turnes its polarity to southward which causes more field lines to be broken and pushed back. As a consequence, the magnetic pressure presses some of the magnetic field lines and force them to reconnect at the sun-away side. The reconnecting magnetic field lines forms a plasmoid which is then translated over the magnetic field lines to the polar caps. During magnetospheric storms and substorm, large amount of energy is transferred to the magnetospheric system.

1.3 Ionosphere

Ionized component of the upper atmosphere is named as the Ionosphere. Ionosphere has important consequences like enabling the flow of currents, effecting the upper atmosphere either by producing or slowing down thermopsheric winds. More important is that Ionosphere

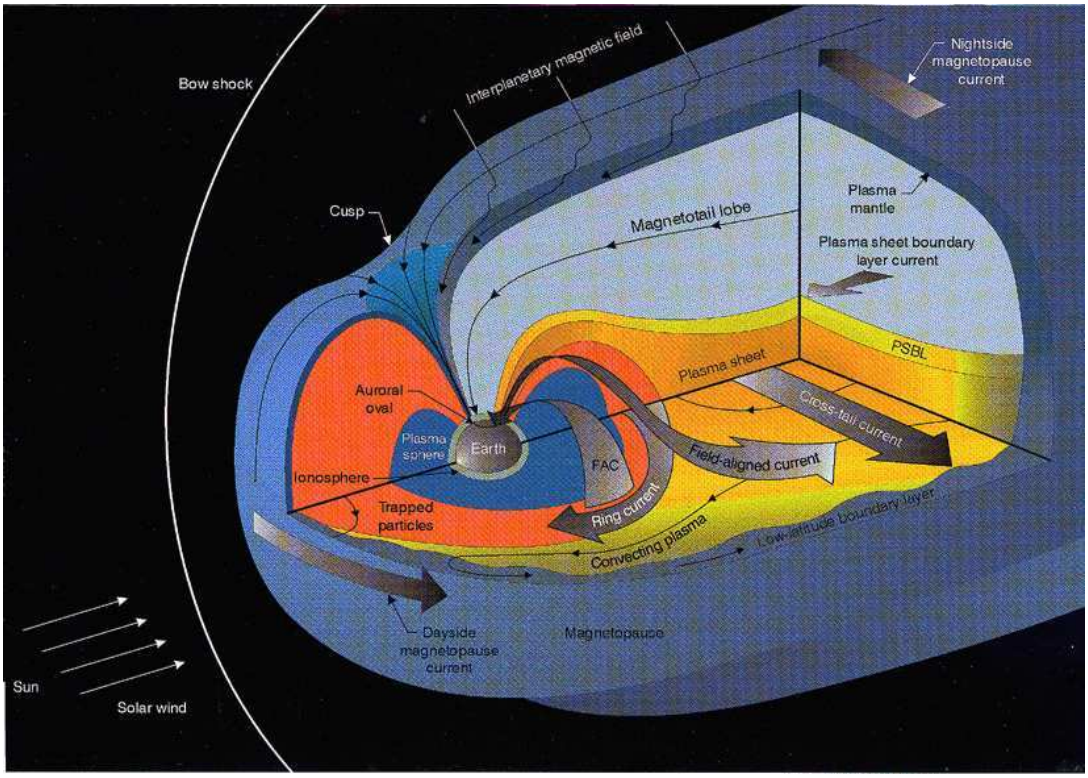

Figure 1.1: The Structure of the Magnetosphere

plays an important role on the modification of the electromagnetic waves[8].

Ionosphere is composed of 3 layers, which are;

- D Layer
- E Layer
- F Layer

These layers are categorized by the chemical reactions taking place, chemical composition and dynamical processes. For more detailed information, the reader is refered to [8] and [14].

From the telecommunication point of view, the most important layer amongst these layers is the F layer since it is the last layer for reflecting the high frequency electromagnetic waves. The maximum frequency which can be reflected from a certain layer of Ionosphere is named as *critical frequency*. Ionospheric F layer critical frequency, f_0F2, which is the maximum frequency of a wave that can reflect from the F Layer, specifies the maximum usable frequency by the relation:

$$f_{usable} = \frac{f_0F2}{sin(\Delta\Lambda)} \tag{1.1}$$

where $\Delta\Lambda$ is the latitude difference between the measurement site of f_0F2 and the position where f_{usable} is calculated. Higher the value of f_0F2 is, higher the f_{usable} is.

At a given time of year and phase in the solar cycle, ionosphere exhibits regular diurnal variations at mid-latitudes as the plasma co-rotates with the Earth. The daily variation of the F region electron density distribution greatly affects the propogation of radio waves in the frequency range from 3 kHz (Very Low Frequencies) to 30 MHz (High Frequency). Of particular importance is the maximum plasma density of the F layer. Since f_0F2 is the important parameter which is (in Hz) numerically equal to about nine times the square root of the maximum electron density (in m^{-3}), unless stated otherwise, the ionospheric variablity was quantified by refering to the f_0F2 values [16]. Thus it is an important and crucial information to know, understand and forecast the value of f_0F2.

1.4 Interaction of Magnetosphere and Ionosphere

Two layers of the Earth, Magnetosphere and Ionosphere are not independent of each other. Processes affecting one of them also effects the other via several mechanisms. Some of the best examples are the Aurora Borealis, Nothern Lights and Aurora Australis, Southern Lights.

Magnetic reconnection at the magnetospheric boundaries in regions where interplanetary magnetic fields are antiparallel and viscous interactions along the boundary makes the energy, momentum and plasma enter the magnetosphere[1]. The Sun's solar energy that is carried by the Solar Wind influences the Ionosphere and Magnetosphere via particles, currents and fields. For more detailed information about the current systems and the connection, reader is refered to [20].

1.5 Literature Survey

The variability greatly limits the efficiency of systems using HF frequencies such as communications, radars and navigation [24, 10]. The possibility that there may be an observable link between the IMF and the behaviour of the mid-latitude ionosphere has led to several investigations [12] and the possible effects of the orientation of the Interplanetary Magnetic Field on Atmospheric, Ionospheric and Magnetospheric phenomena was investigated by many scientists. In [21], the IMF data have been sorted according to the polarity of IMF B_z and studied the effects of the IMF B_z southward turnings on the mid-latitude ionosphere. Following [19], a reversal of the polarity of the IMF B_z component between hourly data points was named as an **event type 1** (with start time t_1 and end time t_2=t_1+1h.) provided that change in magnitude, δB_z, is at least 2 nT. It was required further that the IMF B_z polarity was the same for both 4 h. before and 4 h. after turnings. In total, there were continuous IMF B_z data over an 8 hour period and this condition was met. In order to study the day-to-day variability of the f_0F2 about the regular diurnal variations, each hourly value of f_0F2 *quiet* soundings when simultaneous magnetic Kp index was less than 2+ was identified with 15 days of the sounding in question. Then, the mean quiet-time value at the same Universal Time (UT), the quiet time control value, was subtracted from the actual observed value. The resulting value is then termed as δf_0F2. In [17], [21], it has been pursued the Superposed Epoch (SPE) studies of the f_0F2 values from Uppsala, Lannion, Dourbes, Kalin, Potier, Slough Vertical Ionosondes

and it was revealed that much of the day-to-day variability of the mid-latitude ionosphere may be related to the orientation of the southward IMF B_z. In particular, significant depression of over 1 MHz was found in the average critical frequencies following a southward turning of the IMF B_z.

In [16], the associated geomagnetic response of polarity reversals of IMF B_z by using the SPE method has been investigated since the ionospheric effect is well correlated with geomagnetic disturbance, as seen in a variety of magnetic indices like Kp, AE and Dst when the IMF B_z polarity turned from north to south [16]. It has been confirmed that the energy deposited at high latitudes, which leads to the geomagnetic and high ionospheric disturbances following a southward turning of the IMF, increases with energy density (dynamic pressure) of the solar wind flow[16]. The magnitude of all responses were shown to depend on δB_z

Although, in [25], it has been mentioned that IMF B_y has no significant role on the substorms in their work, many researchers have tried to find a clue of the dependence of IMF B_y on geospace variability. One of the results in [18] proposed a possible relation between the IMF B_y and magnetospheric convection electric field. Moreover, in [13], it has been shown that turnings of IMF B_y during quasi-steady IMF B_z can be linked to the substorm activities. In addition, dependence of auroral activity on IMF B_y and B_x components have been shown by [15]. A more striking and recent result by [5] was that average power flux for both hemispheres was found to be greater for negative values of IMF B_y where power flux in responsible for the photoionization and photodissociation in the Ionosphere. Although, IMF B_z turnings have a crucial effect on the magnetospheric system, it has been shown by [3] that events for which IMF B_z is northward for at least 2 hours before and at least 3 hours after a IMF B_y sign change caused aurora formation in both hemispheres which showed the link between IMF B_y and Ionosphere. Another important effect of IMF B_y is that it modulate the flow pattern of convection via the action of the neutral thermosphere [17].

1.6 Summary

In the space era, the impact of the solar activity on our lives, on the technology, on our past, present and future has to be qualified and quantified. However, processes effecting our system are mostly non-linear and time-varying processes. In complying with such a must, one need

to experiment, monitor, build up Solar and Terrestrial data archieves and do modeling by using the experiences and data available in order to forecast or predict the future for system designers, operators and users.

Therefore, revisiting the problem and including the IMF B_y polarity in the definition of the event, the effects of southward turnings of the IMF B_z were investigated by using Superposed Epoch (SPE) Method. Then the effects of polarity reversals of IMF B_y and IMF B_z components on the f_0F2 for a single vertical ionosonde station were attempted to be modeled by using Genetic Programming Method. It is interesting to note that the SPE has been one of the oldest techniques whereas GP is one of the recent techniques.

CHAPTER 2

DATA

For the analysis, it is required to use geomagnetic indices, which are representatives of geomagnetic activity, and Interplanetary Magnetic Field (IMF) data in addition to f_0F2 ,which is used as a measure of Ionospheric variability, covering 20 years between 1973 and 1993. The geomagnetic data are the 3 hour planetary Kp index and Dst, and IMF which were compiled from SPIDR[1] of the NGDC[2]. The ionospheric data are the f_0F2 values and were compiled from Arkhangelsk (64.4 N; 40.5 E) and Slough (51.5 N; 0.6 W) Vertical Ionosondes.

2.1 Data Used

2.1.1 Interplanetary Magnetic Field

The Interplanetary Magnetic Field data is being measured by IMP[3]. The satellite measures the magnetic fields, plasmas and energetic particles[28]. Interplanetary Magnetic Field being a vector, the satellite measures the magnetic field in three components, one (B_x) of which is in Geocentric Solar Ecliptic (GSE) and two (B_y and B_z) are in Geocentric Solar Magentopsheric (GSM). Detailed information about coordinate systems can be found in Appendix A.

Within the interval of interest, data could only be retrieved hourly, although it was possible to find minutely for the data of more recent years. Due to the reason that all sort of data should be available for the analysis, the interval was selected to be between years 1973 and 1993 and the data frequency was selected as hour..

[1] Space Physics Interactive Data Resource, http://spidr.ngdc.noaa.gov/spidr/index.jsp
[2] National Geophysical Data Centre, http://www.ngdc.noaa.gov/ngdc.html
[3] Interplanetary Monitoring Platform, http://nssdc.gsfc.nasa.gov/space/imp-8.html

The data was organized in such a way that the missing values are flagged with the number $1x10^{33}$ so that the missing values could be extracted easily. The unit used for the magnetic field was nano Tesla (nT).

From the whole dataset, as an example, January of 1973 data were drawn in Figure 2.1. As can be seen from the figure, the IMF values were highly variable.

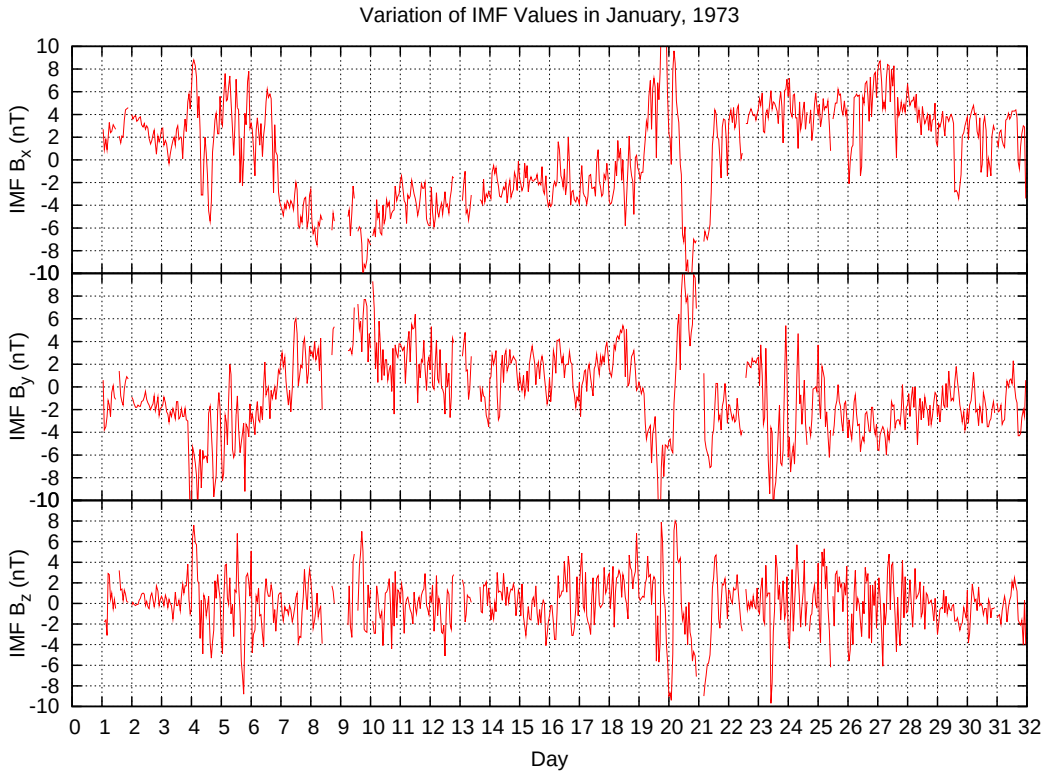

Figure 2.1: IMF Variation during January, 1973

2.1.2 Geomagnetic Indices

Daily regular magnetic field variations arise from current systems caused by regular solar radiation changes. Other irregular current systems produce magnetic field changes caused by the interaction of the solar wind with the magnetosphere, by the magnetosphere itself, by the interactions between the magnetosphere and ionosphere, and by the ionosphere itself. Thus, in order to analyze the variations in the geomagnetic field caused by these irregular current systems, geomagnetic indices were designed[29]. In this work, two of them, most frequently used ones, were employed in order to quantify and qualify the geomagnetic disturbances and

to observe the behaviour of geomagnetic activity during disturbed conditions.

2.1.2.1 Kp

3-h planetary Kp index is a semi-logarithmic scale which is first designed to measure solar particle radiation by its magnetic effects[30]. Kp index is the mean standardized values of 13 different geomagnetic observatories between 44 degrees and 60 degrees northern and southern geomagnetic latitudes[29]. Since the first calculated Kp indices in 1938, there has been no data gap in the databases.

The maximum value of the Kp index is 9 and the values of Kp index are: 1-, 1, 1+, 2-, 2, 2+, 3-, 3, 3+, 4-, 4, 4+, 5-, 5, 5+, 6-, 6, 6+, 7-, 7, 7+, 8-, 8, 8+, 9- and 9. During geomagnetically quiet periods, the value of Kp index is less than 2+. The values between 2+ and 4+ indicates geomagnetically disturbed condition, whereas the values greater than 4+ mean a severe geomagnetic activity.

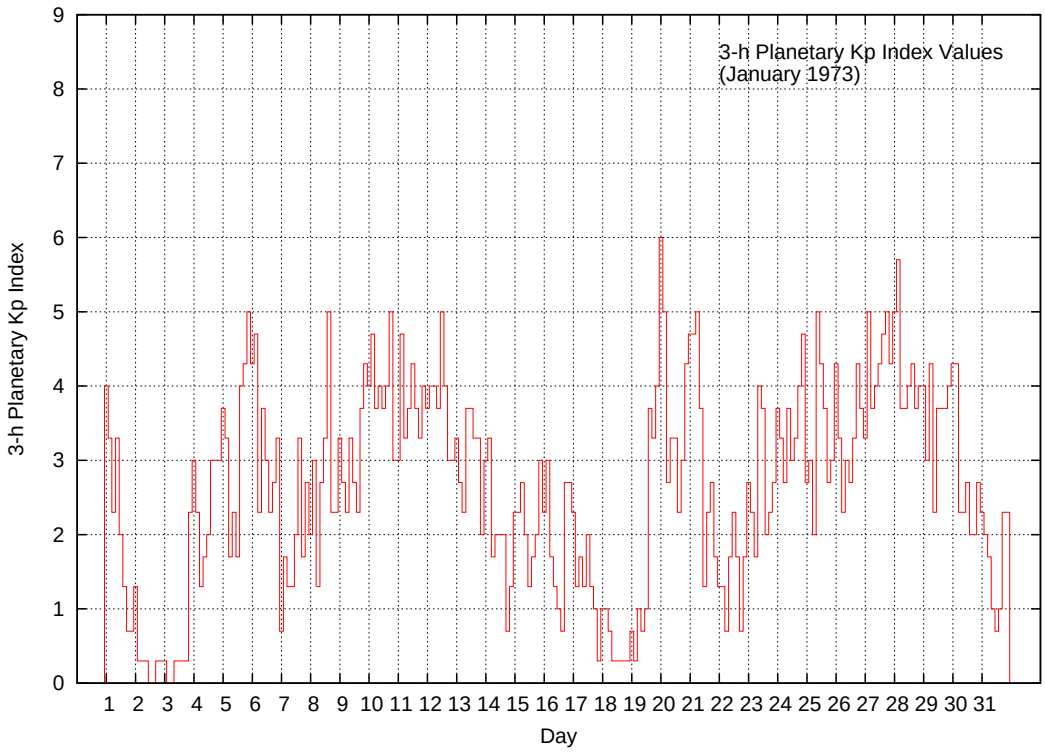

Figure 2.2: 3-h planetary Kp index variation during January, 1973

In Figure 2.2, a sample period was shown. As can be seen from the figure, during January, 1973, it was not much geomagnetically disturbed. Only for 20^{st} and 28^{th} of January, the Kp values have exceeded 4+ and remained at that level for 3-6 hours.

2.1.2.2 Dst

Dst (Disturbance Storm Time) index is the mean of the variations on the horizontal component of the geomagnetic field measured by the near-equatorial geomagnetic observatories. As a consequence of measuring the horizontal components near equatorial, Dst index gives information about the Ring Current activity and the Equatorial Electrojet.

During the geomagnetically disturbed conditions, an enhancement on the ring current density occurs. As a consequence of the enhancement, as a response of the Earth System, the horizontal component of the geomagnetic field is modified. This signature can be seen on the Dst index.

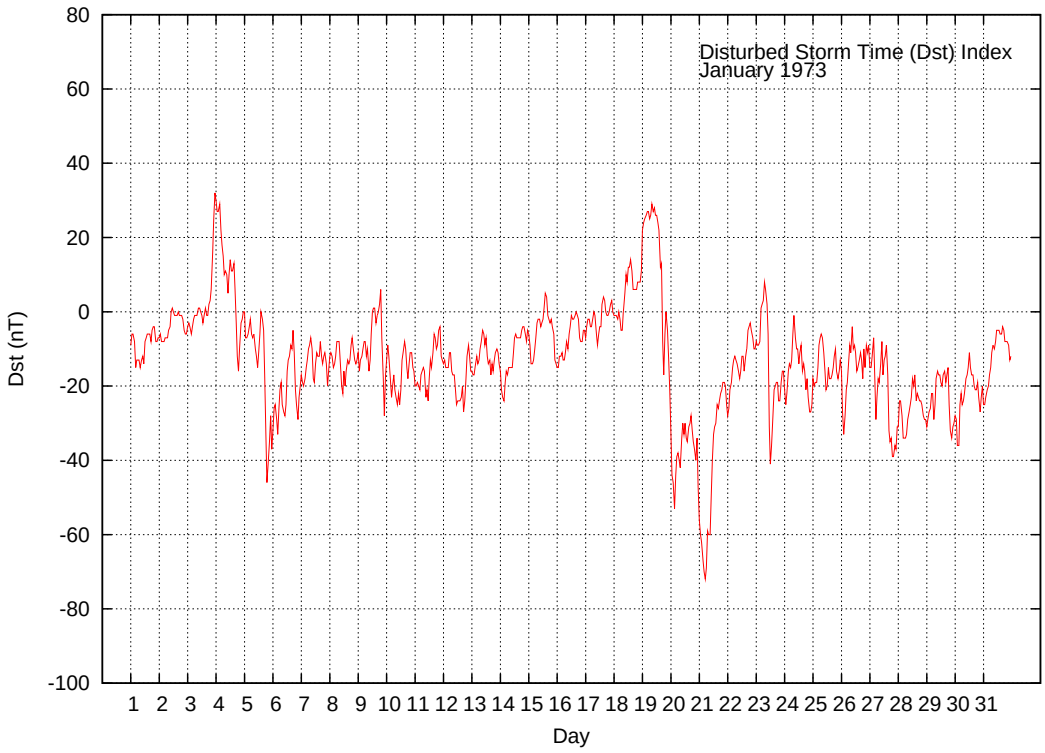

Figure 2.3: Disturbance Storm Time (Dst) index variation during January, 1973

Just after the geomagnetic storm, the accumulation of electrons and protons in the ring current region, the Dst index increases up to certain values. This period is named as the *sudden commencement*. After sudden commencement, the Earth System reacts in such a way to reduce the effect of the accumulation. Thus, after the sudden commencement, the value of the Dst index drops. This period is named as the main phase of the geomagnetic storm. After reaching the minimum value, Dst index starts recovering its original value before the geomagnetic storm, and this phase is called the recovery phase. For more detailed informatio, reader is referered to [8]. In Figure 2.3, the period January, 1973, was shown. The phenomena mentioned above can be easily seen from the figure.

2.1.3 F layer Critical Frequency, f_0F2

F layer critical frequency is the maximum frequency that the Ionospheric F layer can reflect. F layer critical frequency (in MHz) is measured with Vertical Ionosondes which are positioned in many locations, mostly in northern hemisphere. During disturbed conditions the measurements may not be achieved, thus there are data gaps in f_0F2 data, which are flagged as 9999. The Vertical Ionosonde stations of interest have been chosen to be Arkhangelsk, Kerguelen Islands and Slough. However, due to some data gaps in the Kerguelen Islands Ionosonde was excluded for the further analysis.

For the second step of the work, since only one station can be modeled at once, only one station, Arkhangelsk, was used for the modeling using Genetic Programming.

2.2 Data Organization

For the analysis, the data should be quantified, sorted and organized in such a way that the two methods of analysis could be applied with ease. Thus, the data were checked whether there were considerable amount of data gaps or not. In order not to impose any physical meaning by using statistical method (e.g. interpolation, cubic spline, etc) to fill up the data gaps synthetically, the available data were chosen from complete sets. All the data were retrieved from SPIDR of NGDC, and all files retrieved were in the same ASCII format.

CHAPTER 3

SUPERPOSED EPOCH APPROACH

3.1 Method of Analysis

The SPE is a simple statistical analysis technique which is applied to time series. Despite being simple, the SPE is one of the powerful analysis techniques if it is used carefully. The idea was that if you average the data in some clever way in relation to an event, the event signal will remain and all other influences will tend to average out [2]. Thus, the crucial part of applying this technique is to be able to define a proper event definition.

Having defined an event, data of a specifically designated interval were extracted from the complete dataset. Then, the selected data were superposed on each other taking the zero time as the event time. By simply dividing with the total number of identified events, results of SPE were obtained. As prescribed, if the identification of an event representing a physical process succesfully made, the results would reveal dynamic component of the response, or in other words, the information containing component of the response.

3.1.1 SPE Analysis of f_0F2 Values

For the SPE analysis of the F layer critical frequencies, f_0F2, for three different event definitions relying on the magnitude of polarity reversals of IMF B_z and the polarity of IMF B_y were constructed. Since f_0F2 values experience diurnal variation, to eliminate the cyclic behaviour, the diurnal variation of the f_0F2 values for the geomagnetically quiet period (Kp$\leq$2+) was calculated statistically. Subtracting the diurnal variation calculated from the original data yielded the filtered one to a first approximation without any diurnal variation which can be used for the SPE analysis.

Since the purpose was to investigate the influences of the Interplanetary Magnetic Field (IMF), event definitions relied on the changes of the IMF. The events were classified in accordance with the following criteria:

- Event type 1
    1. Southward polarity change
    2. $|\Delta$ IMF $B_z|/\Delta t \geq 6$ to 11 nT/h
    3. IMF B_z Polarity should be same for 3 hours before and after the event
- Event type 2
    1. Southward polarity change
    2. $|\Delta$ IMF $B_z|/\Delta t \geq 6$ to 11 nT/h
    3. IMF B_z Polarity should be same for 3 hours before and after the event
    4. Positive IMF B_y Polarity during the reversal period
- Event type 3
    1. Southward polarity change
    2. $|\Delta$ IMF $B_z|/\Delta t \geq 6$ to 11 nT/h
    3. IMF B_z Polarity should be same for 3 hours before and after the event
    4. Negative IMF B_y Polarity during the reversal period

Table 3.1: Number of Occurances of Events (1973-1993)

$\Delta B/\Delta t$ (nT/h)	Event Type 1	Event Type 2	Event Type 3
≥ 6	216	51	52
≥ 7	159	38	35
≥ 8	112	29	21
≥ 9	86	23	18
≥ 10	67	17	13
≥ 11	50	11	10

Total number of events for all event definitions were tabulated in Table.3.1. The selected data for analysis were the data extracted data from the complete dataset with ±4 days around the event time.

3.2 Results

The number of southward turnings with the change in the hourly IMF B_z values, δB_z, in one hour exceeding a given value for the years 1973 to 1993 was shown in Figure 3.2. Superimposed on the same reference frame, the number of southward turnings with IMF $B_y > 0$ and IMF $B_y < 0$ during the event time of 8 hours were also shown. From this figure, it can be seen that over 190 turnings with δB_z = 2 nT/h; 40 turnings with δB_z = 6 nT/h; 12 turnings with δB_z = 11 nT/h. In order to define and quantify the ionospheric and geomagnetic responses to these IMF changes as clearly as possible, $\delta B_z \geq 6$ nT/h and $\delta B_z \geq 11$ nT/h events were selected. This enabled to investigate the effect of varying the threshold of δB_z on the ionospheric and geomagnetic parameters. Then, the **event type 1** definition was revised to include the IMF B_y polarity. Summarizing, the **event type 2** was refered to IMF $B_y < 0$ and the **event type 3** was refered to IMF $B_y > 0$ both 4 hours before and after the southward turning of IMF B_z.

As presribed in Section 3.1, to apply the SPE Method to δf_0F2, diurnal variation of f_0F2 were calculated and subtracted from the original data, so that refined data without daily variations could be obtained. In order to calculate the diurnal variation, as prescribed in Chapter 3.1, by averaging the geomagnetically quiet hourly values of f_0F2 15 days around an event, diurnal variation of f_0F2 was obtained, and for $\delta B_z \geq 6$ nT/h case, the diurnal variation was shown in Figure 3.1.

In the Figure 3.2, 3.3, 3.4, 3.5, the probabilities and cumulative probabilities of δf_0F2 for Vertical Ionosnde Arkhangelsk, Dst and Kp were also plotted. It can be seen that, although dialy variations were excluded, the probability of having f_0F2 equal to approximately -1 was maximum. This was due to the tendency of events to mostly happen at a certain time, yielding a peak slightly translated from the zero point.

Different than the case for f_0F2, the Dst index had its maximum probability near zero. This showed that Dst index do not have a daily variation like f_0F2. For the probability of 3 hour planetary Kp index, the maximum probable value was found to be approximately 2. Since 2+ value of Kp designates as the limit between quiet and disturbed conditions, probabilities calculated confirmed the designated value.

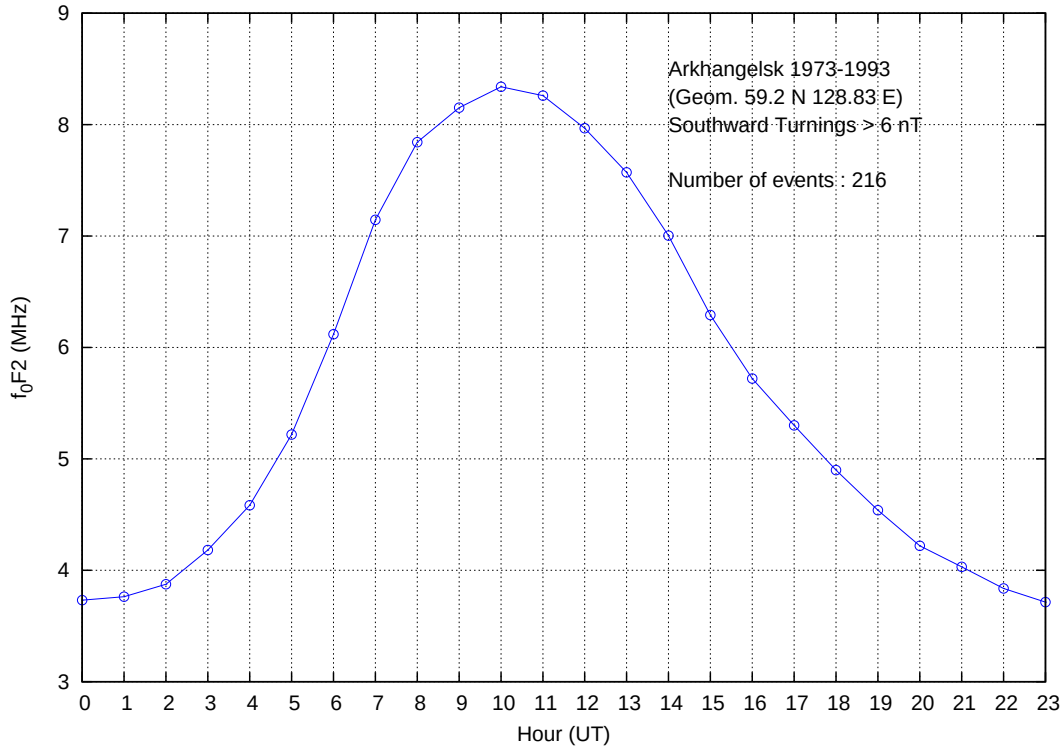

Figure 3.1: Diurnal Variation of δf_0F2 for Arkhangelsk Vertical Ionosonde

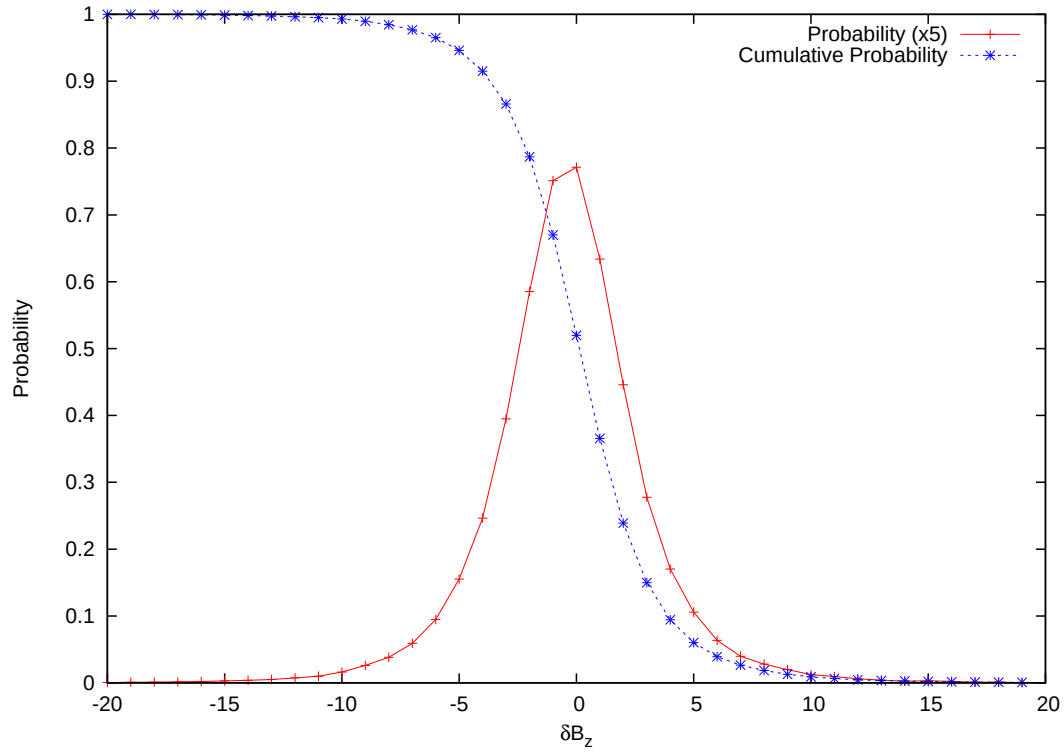

Figure 3.2: Probabilities and Cumulative Probabilities of IMF B_z

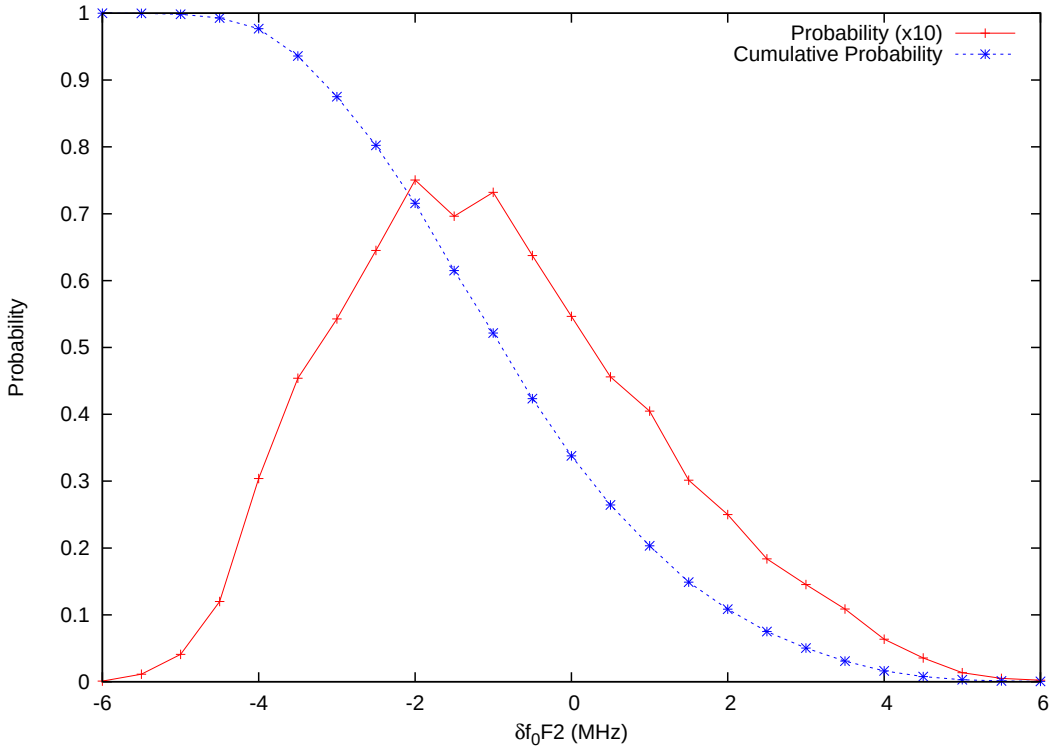

Figure 3.3: Probabilities and Cumulative Probabilities of f_0F2 values

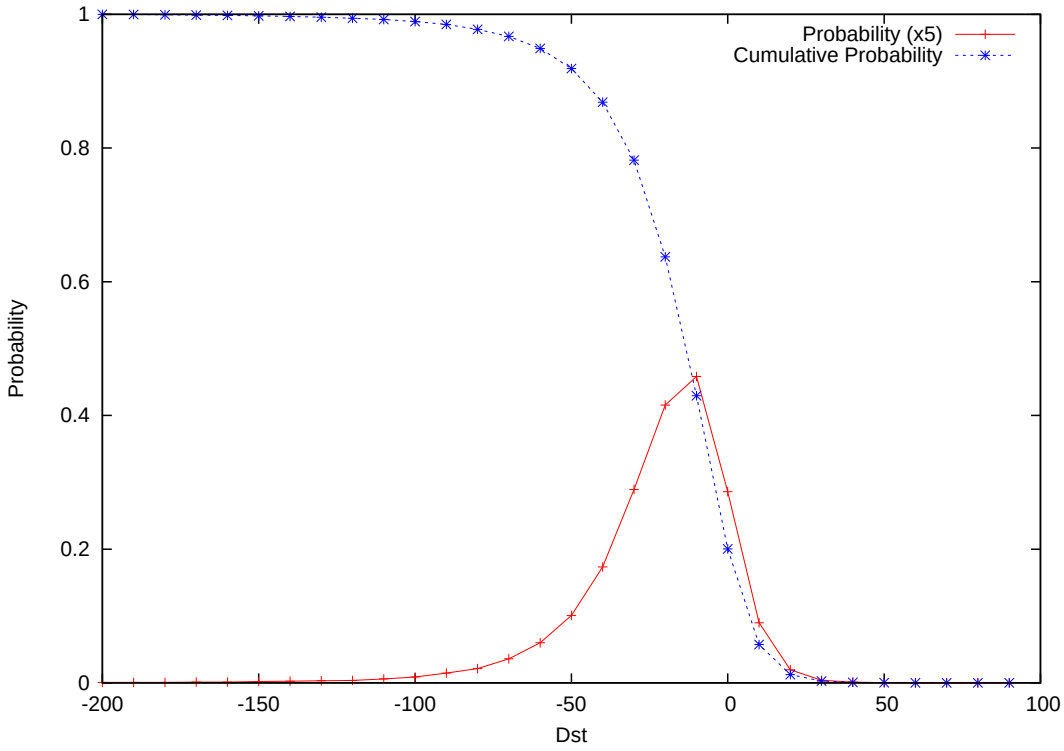

Figure 3.4: Probabilities and Cumulative Probabilities of Dst index

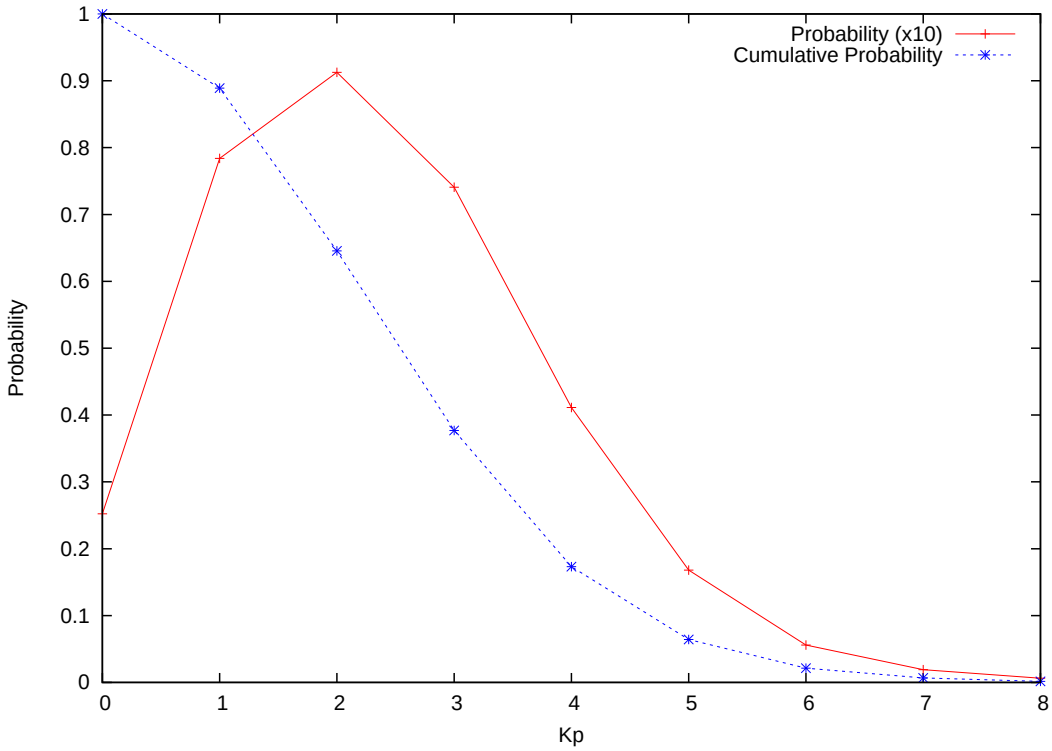

Figure 3.5: Probabilities and Cumulative Probabilities of Kp index

To be able to quantify the results, method was applied twice, which was first applied only for the IMF B_z reversal cases and the second was for the IMF B_z reversals with the IMF B_y criteria.

3.2.1 Superposed Epoch Analysis Results for IMF B_z reversals

3.2.1.1 Effects on Geomagnetic Activity

The geomagnetic response to the Interplanetary Magnetic Field variations could be traced from the geomagnetic indices. Thus, the SPE Method was applied to geomagnetic indices to reveal the response of the geomagnetic activity to IMF reversals.

Effects on Kp The effect of IMF B_z reversal on the 3 hour planetary Kp index was shown in Figure 3.6. The peak value of Kp was achieved approximately 3 hours after the zero time which was the event time.

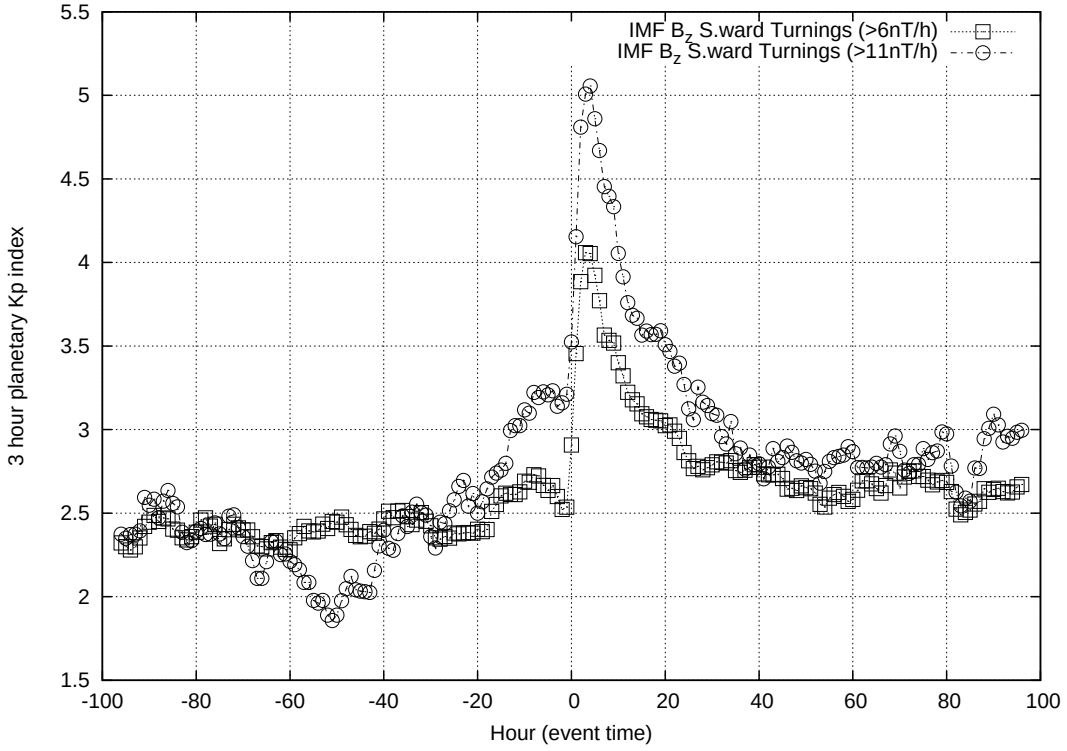

Figure 3.6: SPE Results of Kp index for southward turnings with $\delta B_z \geq 6$ nT/h and ≥ 11 nT/h

Kp index increased rapidly up to 4 and 5 for ΔIMF $B_z/\Delta t \geq 6$ nT/h and ΔIMF $B_z/\Delta t \geq 11$ nT/h,

respectively. Two third of both cases were achieved ~20 hours after the zero time. These results were correlated with the ones computed by [16]

Effects on Dst The effect of IMF B_z reversal on the Dst index was shown in Figure 3.7. The peak value of Dst was achieved approximately 7 hours after the zero time which was the event time.

Dst averages about 15 nT and 19 nT before the event time in the previous 4 days and at the zero hour, Dst increases and it decreases rapidly to values as low as -40 nT and -60 nT for for $\delta B_z \geq 6$ nT/h and for $\delta B_z \geq 11$ nT/h, respectively. This represents a significant enhancement of the ring current. Two third of both cases were achieved ~20 hours after the zero time. These results were correlated with the ones computed by [16]. This was also correlated with the results obtained for the SPE results of Kp index.

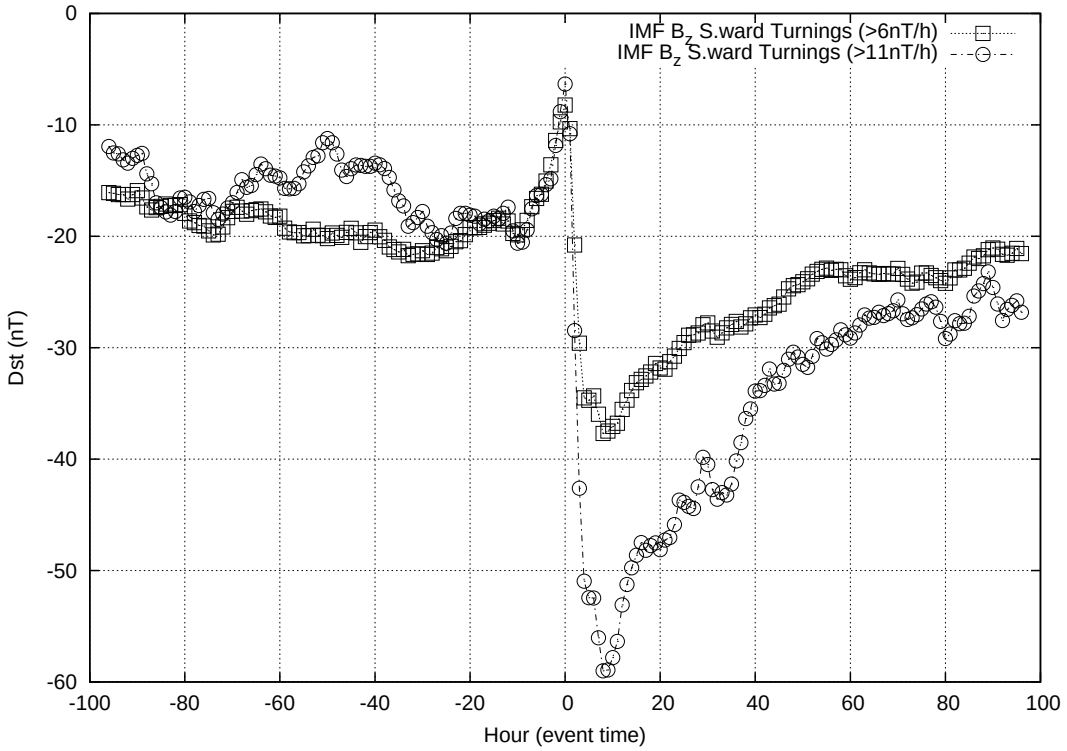

Figure 3.7: SPE Results of Dst index for southward turnings with $\delta B_z \geq 6$ nT/h and ≥ 11 nT/h

3.2.1.2 Effects on F layer Critical Frequency, f_0F2

The signal of Ionospheric variability as a response to the IMF reversals were also observed and plotted in Figures 3.8 and 3.9. Although there were small fluctuations before the event, after the zero time, event time, there was a sudden decrease in the value of δf_0F2, which was the signal of the IMF reversal signal. For both stations, Arkhangelsk and Slough, similar to geomagnetic indices, the values suddenly change and have their minimum values ~20 hours after the event, with the values -1.1 MHz and 1 MHz for Arkhangelsk and Slough, respectively.

Although there needs more detailed inspection, there should be a link between the decaying phases of f_0F2 and geomagnetic indices, since δf_0F2 achieved its minimum value at the time when the geomagnetic indices achieved their one third of their maximum values.

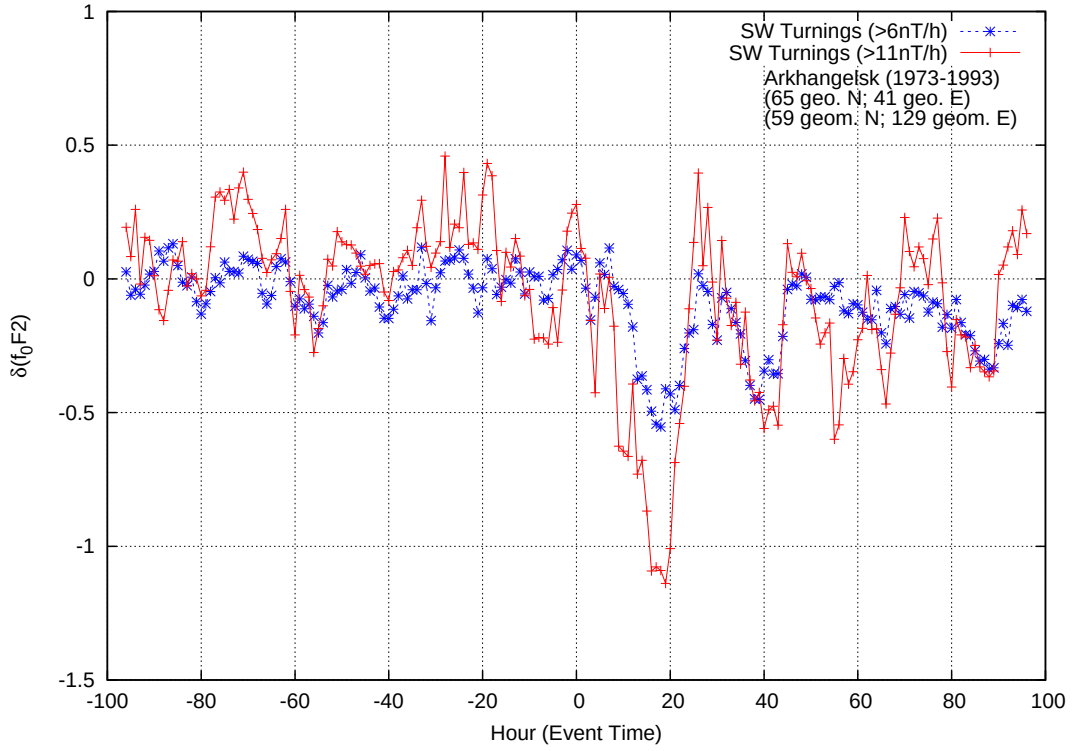

Figure 3.8: SPE Results for southward turnings with δB_z ≥6nT/h and 11nT/h for Arkhangelsk

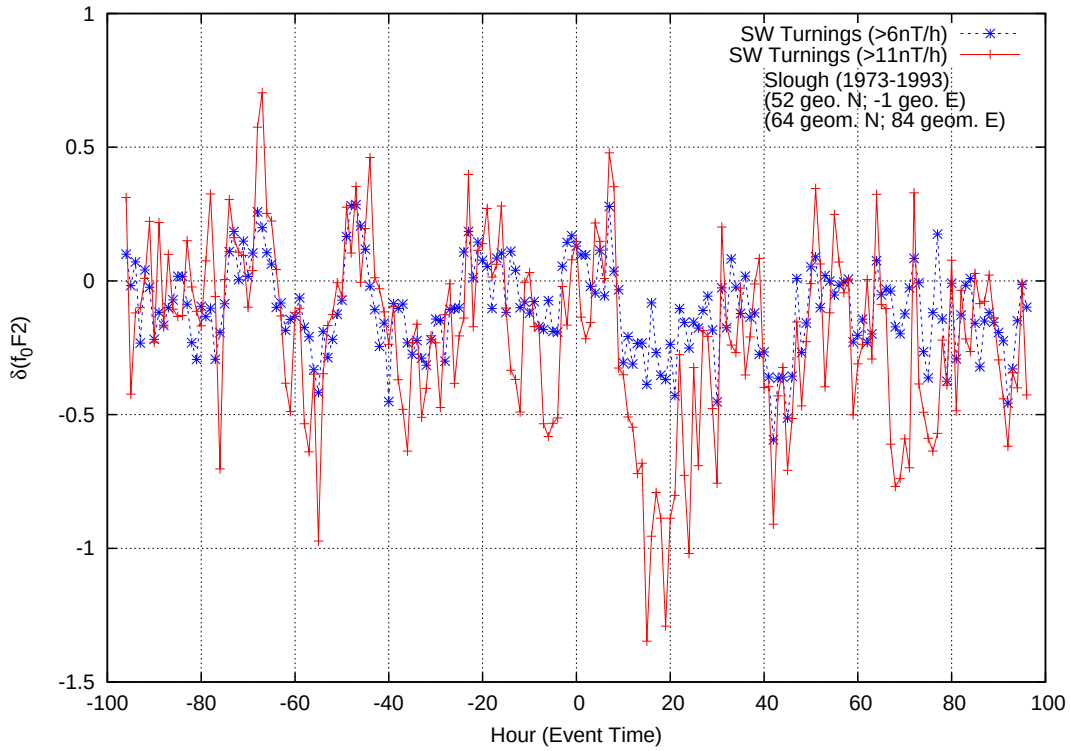

Figure 3.9: SPE Results for southward turnings with $\delta B_z \geq$6nT/h and 11nT/h for Slough

3.2.2 Superposed Epoch Analysis Results for IMF B_z reversals during Steady IMF B_y Polarity

3.2.2.1 Effects on Geomagnetic Activity

Effects on Kp SPE Method showed that there was no significant difference for the events of $\delta B_z \geq$6 nT/h. These results were plotted in Figure 3.10. As in the case of results obtained for the event type 1, the maximum value was 4 which was observed at 3 hours after the zero time.

However, as the magnitude of the reversal as increased to 11 nT/h, the IMF B_y signal became observable which be seen in Figure 3.11.

It was interesting to note that 3 hour planetary Kp values increases before the zero event time and remain relatively at high values for 20 hours after the zero event time when IMF B_y >0 throughout the 4 day period.

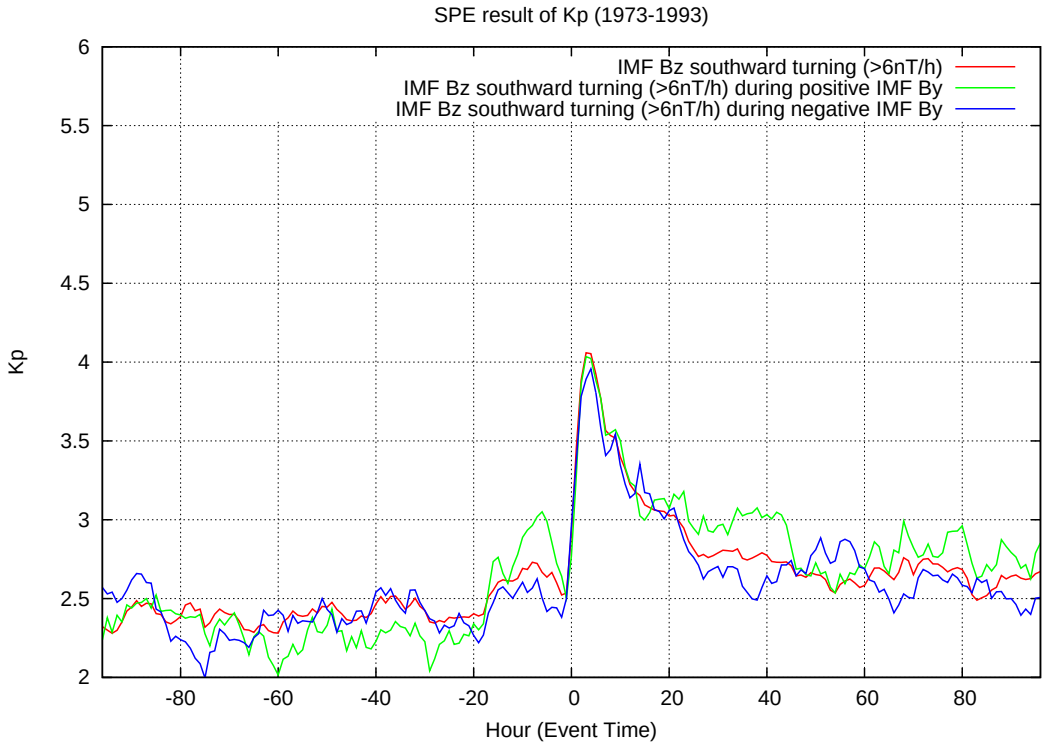

Figure 3.10: SPE Results of Kp index for southward turnings with $\delta B_z \geq 6$nT/h for three IMF B_y criteria

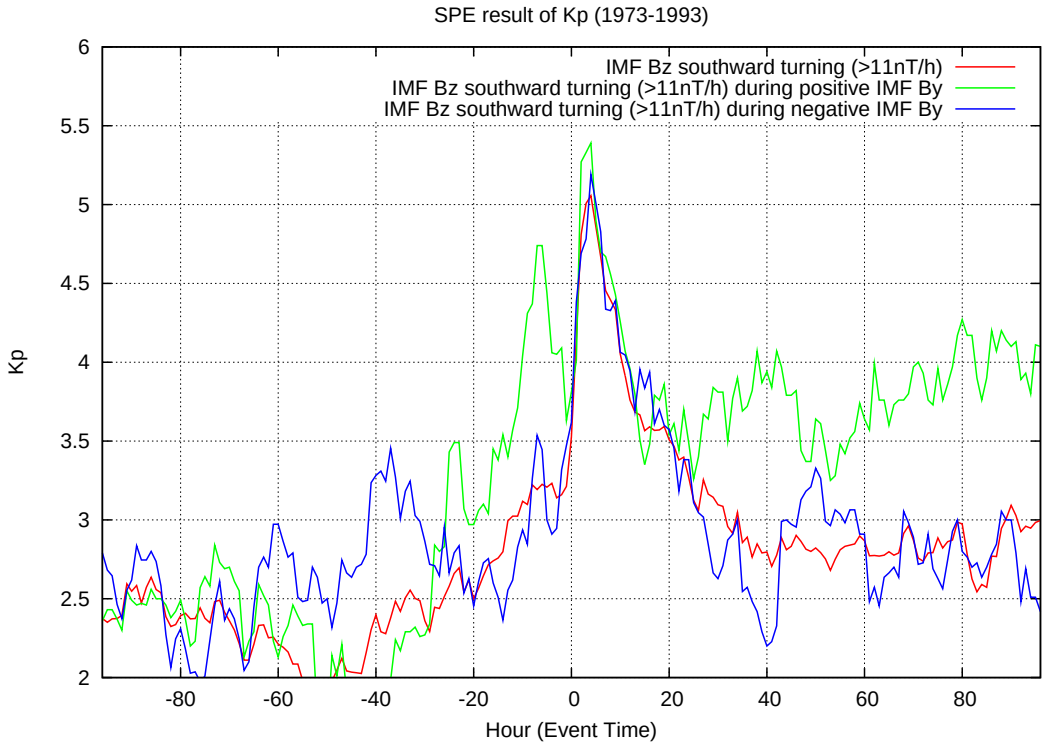

Figure 3.11: SPE Results of Kp index for southward turnings with $\delta B_z \geq 11$nT/h for three IMF B_y criteria

Effects on Dst As effects on the Kp index, there was not much significant difference between three event definitions.

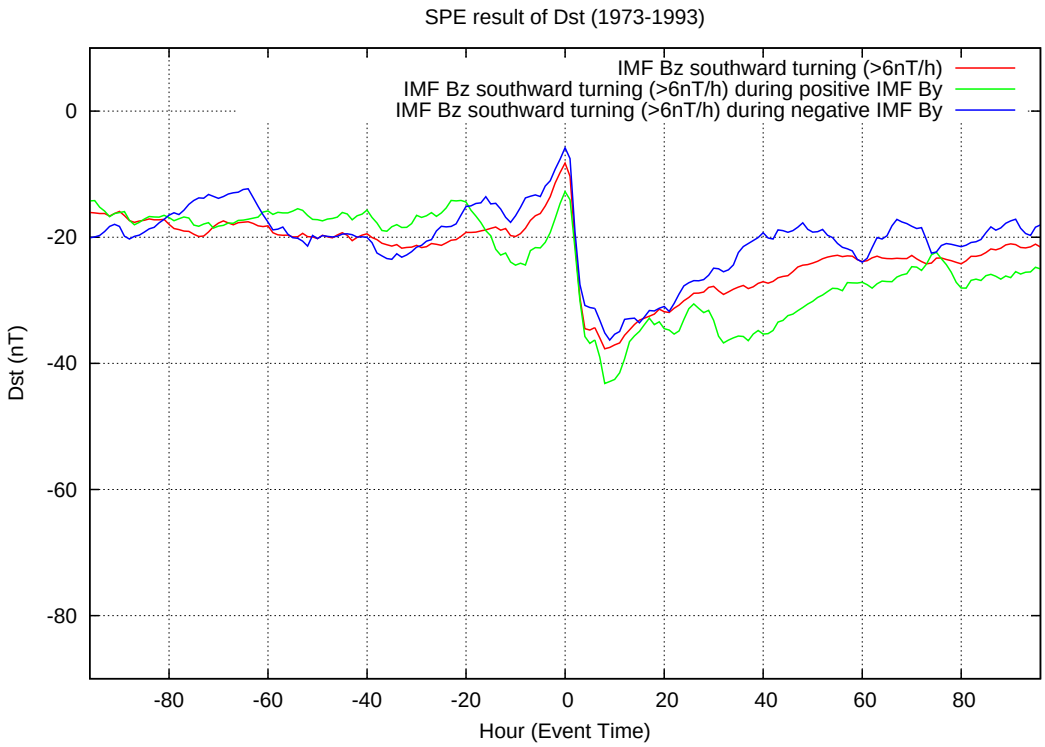

Figure 3.12: SPE Results of Dst index for southward turnings with $\delta B_z \geq 6$nT/h for three IMF B_y criteria

In the case of the Dst values, following the zero time, the Dst values remain relatively at low values for the IMF $B_y > 0$ polarity during the 4 day period after the zero event time. Moreover, it can be interpreted that the positive IMF B_y was continued more than 3 days which indicates the continuation of enhanced ring current activity.

3.2.2.2 Effects on F layer Critical Frequency, f_0F2

It was interesting to note that after the IMF B_y criteria switched on, the southward turnings of the IMF B_z, the SPE results of δf_0F2 values of event 2 and event 3 seem to exhibit a symmetrical bahaviour with respect to the δf_0F2 values of event type 1 within the first 20 hours after the zero event time. In addition to this apperance, the δf_0F2 values after the zero event time were very similar for the event type 1 and event type 2 cases.

With the limitations that f_0F2 values were not continuous indefinitely as the geomagnetic

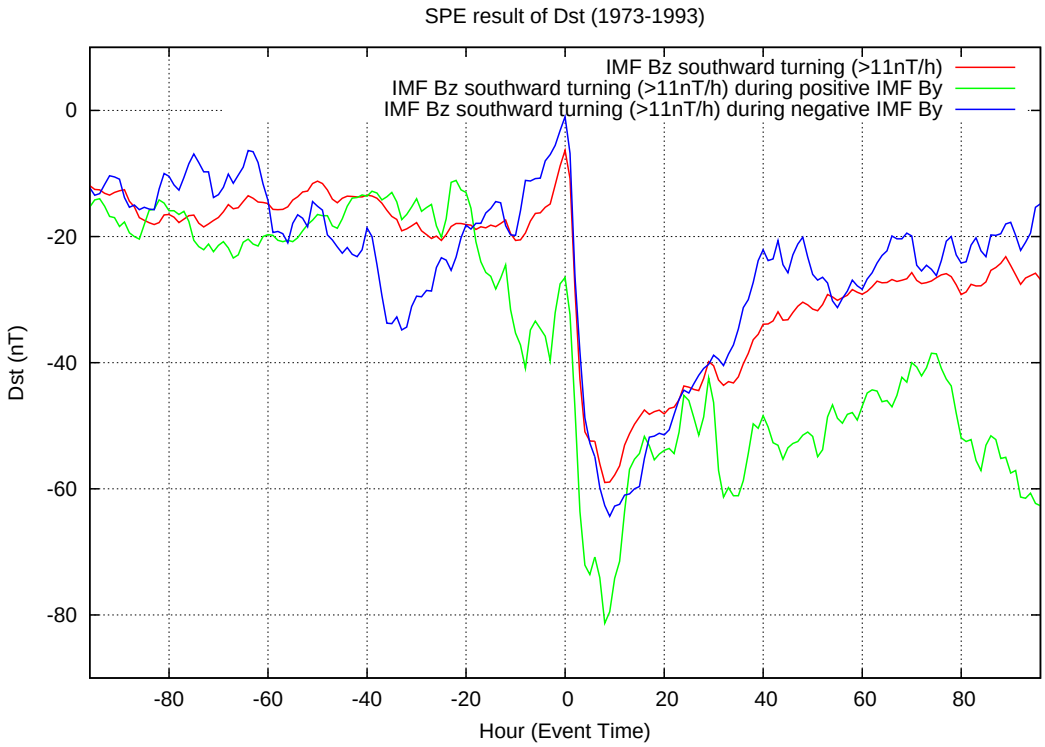

Figure 3.13: SPE Results of Dst index for southward turnings with $\delta B_z \geq 11$nT/h for three IMF B_y criteria

indices during event times, the event 2 and event 3 criteria could not be met with significant number of event cases. Thus, the analysis could not be carried out with these criteria using Superposed Epoch Method.

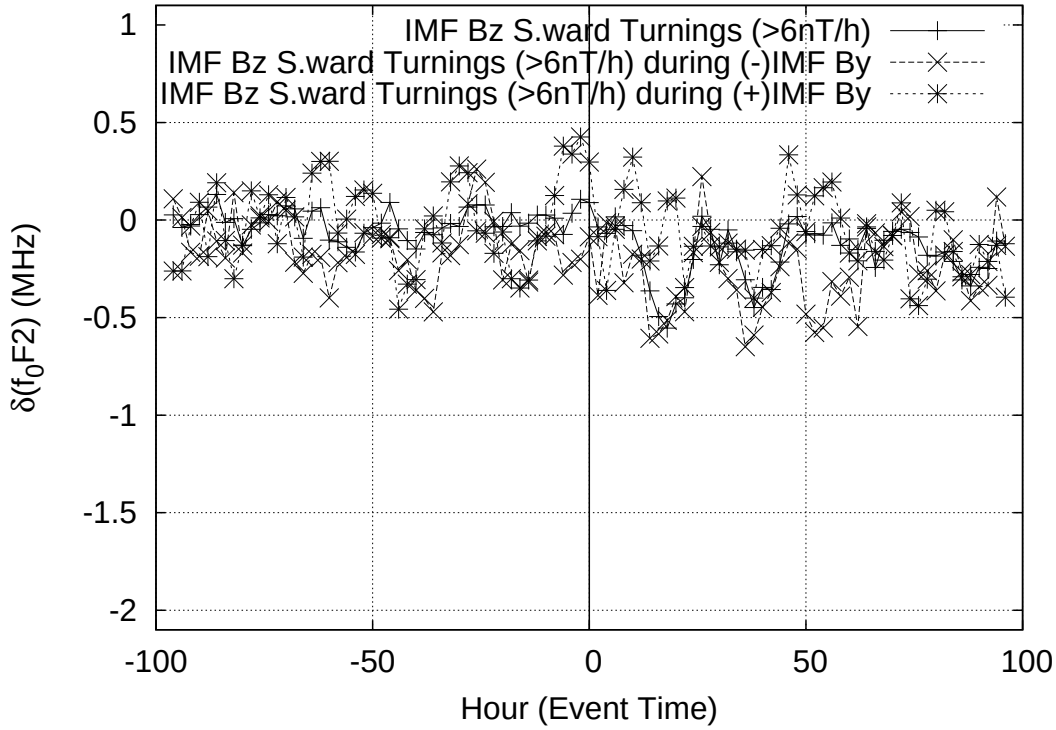

Figure 3.14: SPE Results of f_0F2 for southward turnings with $\delta B_z \geq 6$nT/h for three IMF B_y criteria

CHAPTER 4

GENETIC PROGRAMMING APPROACH

4.1 Method of Analysis

The GP is a powerful algorithm among the family of evalutionary computational methods. The GP is based on the biological evolution of the computer programs resulting in an optimum mathematical model of the system.

“For the conventional genetic programming, the structures undergoing adaptation is a population of individual points from the search space, rather than a single point. Genetic methods differ from most of the other search techniques in that they simultaneously involve a parallel search involving hundreds or thousands of points in the search space.”[23]

As in the biological evolution, computer programs (individuals) whose result best fits the observed values, the succesful ones, can survive as they are, whereas unsuccessful individuals are crossed over or mutated. As can be understood from the statement above, the operations taking place in the GP are reproduction of best fitting individuals, crossing over of individuals with lower fitness and mutation of remaining unsuccessfull individuals.

Each function taking part in the Genetic Programming is named as an individual. The characteristics of an individual is represented as a tree structure which is shown in Fig.4.1 as opposed to the characteristics of human, DNA, which is also shown in Fig. 4.2.

A node of an individual is a joint in a tree structure. A terminal point is the node that the mathematical operation are executed. For ease of use, an arm is named as a tree structure under a node.

For the creation of individuals and generations in the process, a certain set of function to be

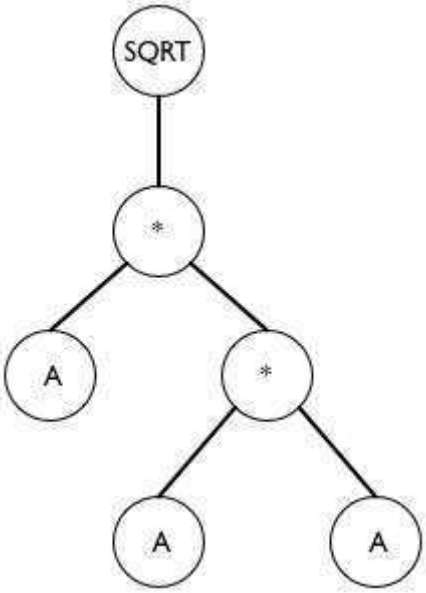

Figure 4.1: A sample tree structure of an individual

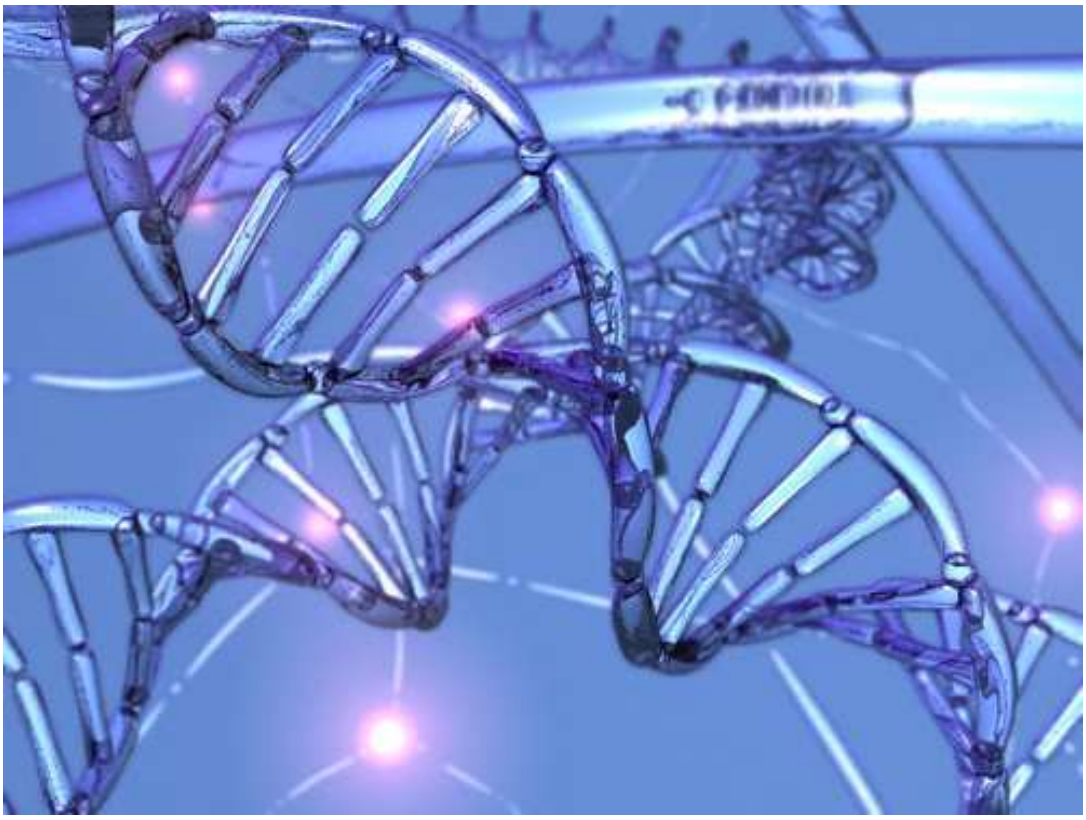

Figure 4.2: Deoxyribonucleic Acid (DNA)

used at terminal points should be created. Depending on the problem of interest, the number and type of the functions are determined.

4.1.1 Operators

In order to obtain of new generations, some operators should act on individuals. Analoguous to biology, individuals will reproduce, crossover with each other or can mutate. Certain fractions of generation with high fitness with respect to other individuals are reproduced to next generation to carry the fitness information to the next generation. Some fraction of the generation with less fitness are crossed over to create more successful individuals fitting the requirements. The remaining fraction of the generation, unsuccessful individuals that should not survive anymore, are mutated. Although in biological situation, most of the time, mutation does create individuals with defects; for GP case, it is assumed that there cannot be any individual worse than the un-mutated individual. In addition, for some cases, mutation results in a jump in the evolution of individual, increasing overall fitness of generation.

From a computer program perspective, the operators can be defined as follows:

- Reproduction

  An individual with a high fitness is passed to next generation without any change.

- Crossover

  Crossover is applied on an individual by simply switching one of its nodes with another node from another individual in the population. (Fig.4.3, Fig.4.4)

- Mutation

  Mutation does not involve any pairs, but it affects an individual in the population. It can replace a whole node in the selected individual, or it can replace just the node's information.

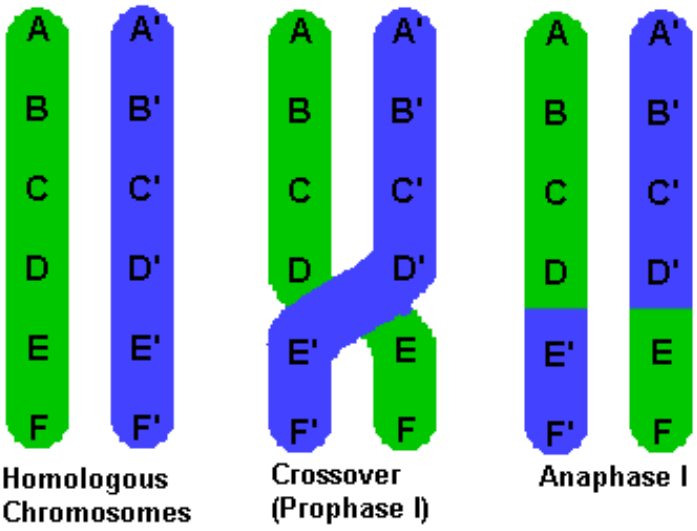

Figure 4.3: The crossing-over process for human DNA

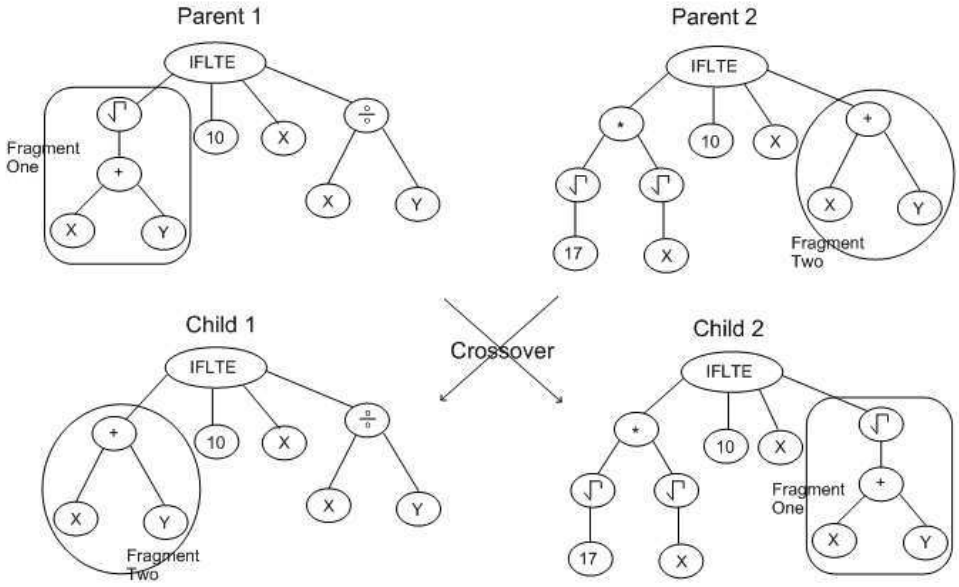

Figure 4.4: A sample crossing over operation

4.1.2 Function Sets

As described above, the terminal points are the points where the mathematical functions are executed. For every individual of the generation of interest, there should be some certain number of terminal points to exist. The choice of a function set for the GP is mostly dependent on the structure of the problem to be solved. For example, if one is given a simple dataset of a polynomial, intuatively, the system can be solved by simple algebraic functions, F={+, -, *, /}. For more complex input/output relations, some other functions like trigonometric, power or exponential functions should be employed. However, unless a small tree of individual is assumed, exponential functions and power functions are useless. Such functions cause *floating point over-flow* error, since the depth of tree gradually increases the numbers to evaluate.

In addition to the simple algebric and trigonometric functions, F={+, -, *, /, sin, cos}, some specially introduced functions can be added to the function set.

4.1.3 Creating Initial Generation

There are various techniques of creating an initial generation. These are “full”, “grow” and “ramped-half-and-half” generation techniques. In full generation technique, all arms of the trees of the individuals are extended to a certain depth specified by the user. For the grow generation technique, all the arms of the trees of the individuals are not to be extended to a certain specified depth specified by the user, but at least one arm of the tree is ought to extend to the maximum depth. The ramped-half-and-half method is just a combination of the previously described methods.[23]

4.1.4 Creating Initial Individuals

The initial individuals are constructed using a random number generator. Depending on the inputs, maximum depth for new individuals, function set and generation technique, functions were placed at the nodes of tree structure without exceeding the specified maximum depth for new individuals.

4.1.5 Generations and Error Analysis

At each generation the individuals were sorted in accordance with their fitness to observed values. Fitness, for this work, was defined as the normalized relative error which is:

$$\text{Norm. Err.} = \frac{1}{N}\sum_{1}^{N}\frac{\|\text{Observed Value - Computed Value}\|}{\text{Observed Value}} \tag{4.1}$$

where N was the number of data used in testing.

The best fitting individuals were reproduced, and less fitting ones are crossed-over. The remaining worst individuals were mutated. This procedure was repeated until the convergence criterion, which corresponds to a normalized relative error of 2.5%, has been met or the maximum number of generation has been achieved.

4.1.6 Genetic Programming for f_0F2 Values, GETY-IYON

Since response of the Ionospheric variability could not have been shown easily for the IMF B_y events, a different method, Genetic Programming (GP) approach was employed. Shortly, the GP was employed to model the probable effects of polarity reversals of IMF B_y and B_z components on the f_0F2 variability. Thus, event definitions have been modified such that only polarity reversals of IMF B_z and IMF B_y were taken to be seperate and independent events. Depending on these events, GP was used and four independent models were constructed. In order to characterize the eventless periods, one more model was constructed.

In order to have maximum changeability while applying GP, a Genetic Programming code was written in GNU OCTAVE, which is an open source project that can replace the MATLAB and the name of the code was given Genetic Programming by Tolga Yapıcı, GETY.

4.1.6.1 Construction of Models

The input parameters of constructing models were the maximum number of population, size of population, fractions of reproduction, crossover and mutation. Best values for these pa-

rameters were obtained by trial-and-error method. The maximum number of population and size of population were kept constant for the construction of all models and the values were:

- Maximum number of populations: 200
- Size of population: 200
- Fraction of Reproduction : 20%
- Fraction of Crossover: 70%
- Fraction of Mutation: 10%

However, since the generation of initial individuals relies on random number, the same results cannot be obtained.

From the classical GP point of view, the mutation is applied to the individuals that have the worst fitness values. However, in the code GETY, the mutation definition was changed. In the mutation definition, the best fitting individuals were copied over the worst ones as well as being reproduced and the copied individuals were mutated. By this way, the GETY code did also worked as a simple optimization tool.

The input variables for constructing the models were the three consecutive values of IMF B_y, IMF B_z and f_0F2. In order to carry the polarity change information for the next hours, a special technique was applied. The code altered the IMF data in such a way that only the magnitude and the polarity change of the IMF B_y and IMF B_z entered in the GETY code. Except the times of polarity reversal change, the IMF data entering the system was given as 0 (zero). For the times of polarity change, the magnitude of the polarity change were given to the GETY as an input. Then, in order to carry the information of polarity change, linearly decaying values of polarity change were given to GETY. By this way, the GETY could apply the polarity change effect for the post-event times. For the values of f_0F2, Arkhangelsk Vertical Ionosonde data were considered. The data covers a period of years 1973 to 1993. The dataset was seperated into two distinct sets. One of the dataset (1973-1980) was used in order to construct the model, whereas the second dataset (1980-1993) was used in order to test the model. The first data group was also seperated in 5 different groups, which were the inputs of each model and polarity reversals of IMF B_y and B_z.

For the critical value of polarity change, relying on the statistical results obtained in previous part, a polarity change greater than 6 nT/h was selected. Thus, for each polarity reversal case, distinct models were constructed. In total, five models were contructed which are:

- Model 1: Model with all inherent event definitions
- Model 2: Model for S.ward IMF B_z polarity reversals greater than 6 nT/h
- Model 3: Model for N.ward IMF B_z polarity reversals greater than 6 nT/h
- Model 4: Model for E.ward IMF B_y polarity reversals greater than 6 nT/h
- Model 5: Model for W.ward IMF B_y polarity reversals greater than 6 nT/h

Also the structure of the model was represented in Fig.4.5

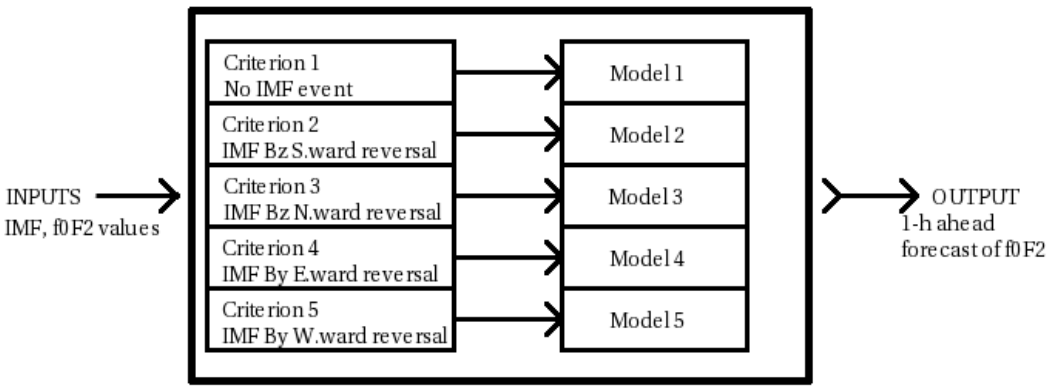

Figure 4.5: Structure of the GETY-IYON

4.2 Results

In Table 4.1, the normalized errors of the seperate models were shown. The high values of error for the Model 1 and Model 2 were the results of the dominance of other events in the interval of interest. However, when one merges 5 models into a single model, then the relative error reduces to 7.3%. This combined model was named as GETY-IYON and the

Fig.4.5 illustrates the working principle of the combined model. In Figure 4.6, observed and computed values of f_0F2 using GETY-IYON and Sunspot Numbers was shown. As can be seen from the figure, the variation of the values of f_0F2 exhibit the dependence on Solar Cycle, which was interpreted from the Sunspot Numbers. As previously described, the data covers two solar cycles which were 1973-1983 solar cycle (used for contructing the models) and 1983-1993 solar cycle(used to test the performance of hte model GETY-IYON). In order to justify the results, results of two selected years which correspond to solar maximum and solar minimum were also ploted.

Table 4.1: Relative Errors of 5 seperate GETY models

	Model 1	Model 2	Model 3	Model 4	Model 5
Normalized Error (%)	17.3	17	9.3	11.2	10.7

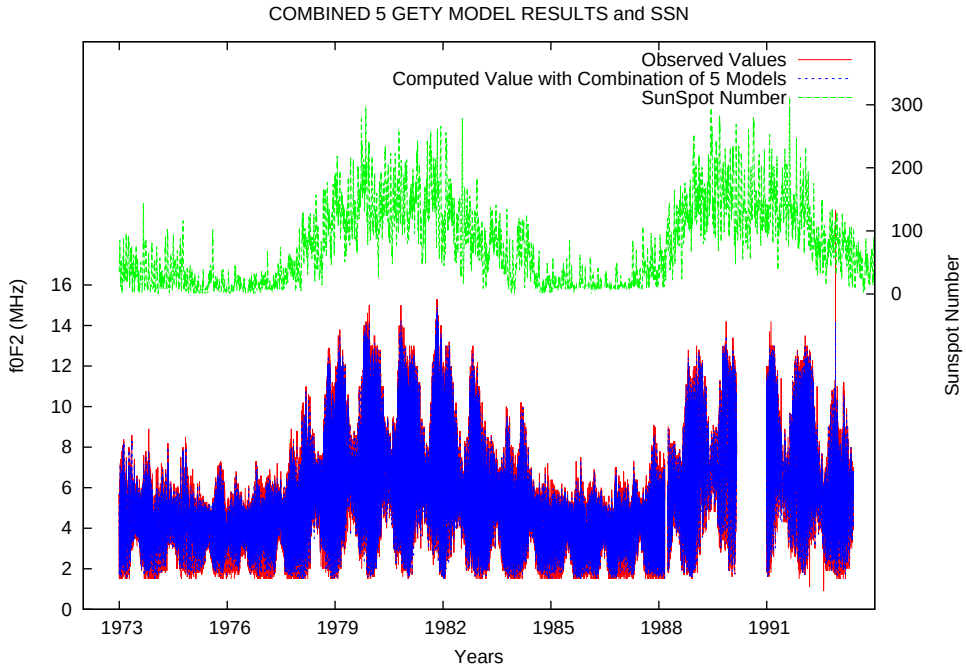

Figure 4.6: Observed Values (in red) and Genetic Programming Results (in blue) of f_0F2 values and the variation of Sun Spot Number

As can be seen from the figures below, the model values well correlated with the observed values at the significance level of 90%. For interpreting the results, next, an extended analysis has been conducted by considering seasonal and monthly data during 1982 and 1987.

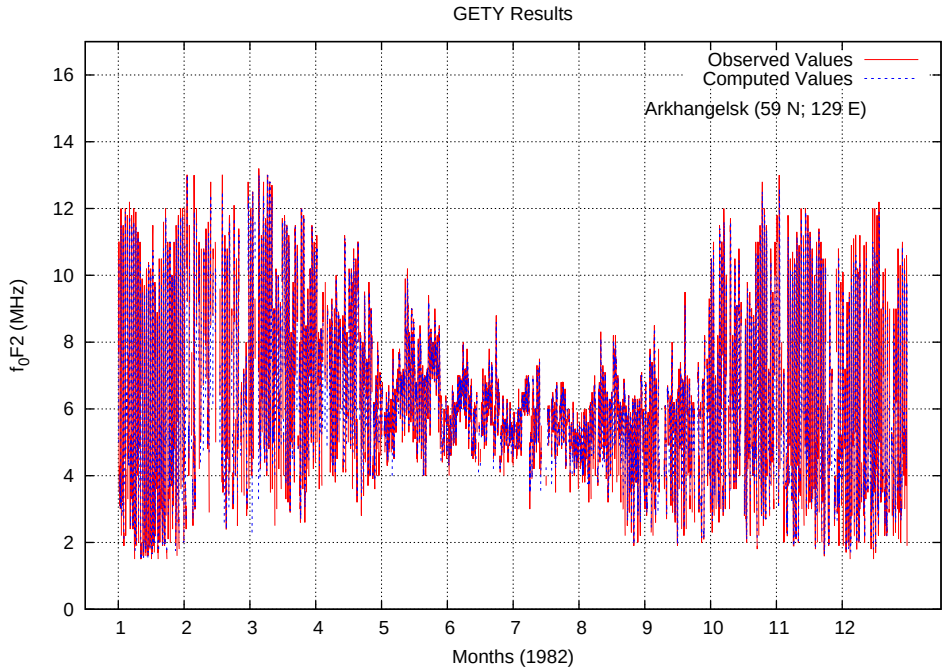

Figure 4.7: Observed Values (in red) and Genetic Programming Results (in blue) of f_0F2 values for the year 1982

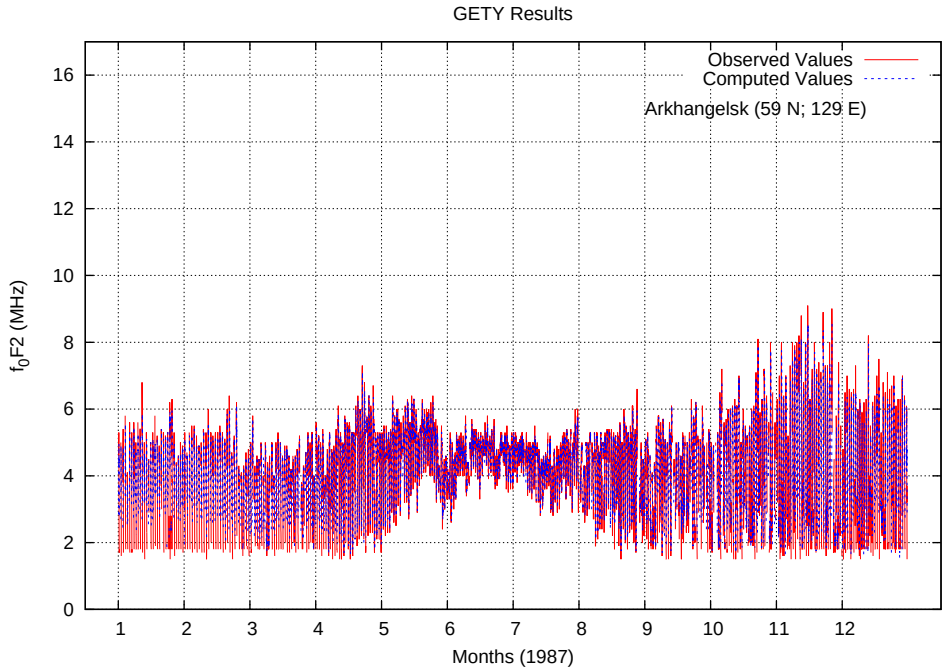

Figure 4.8: Observed Values (in red) and Genetic Programming Results (in blue) of f_0F2 values for the year 1987

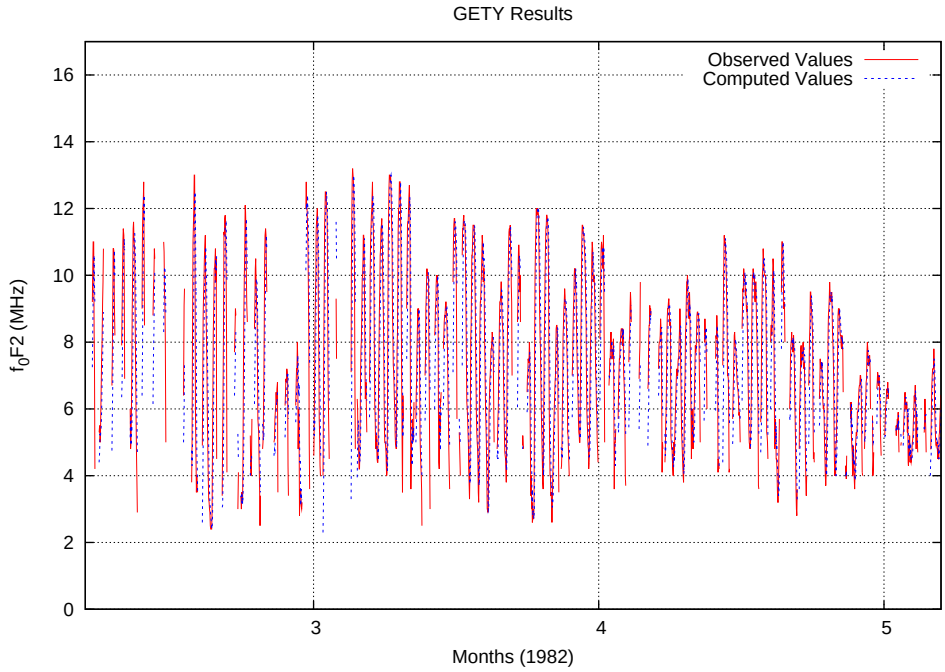

Figure 4.9: Observed Values (in red) and Genetic Programming Results (in blue) of f_0F2 values for the year 1982 around Spring (Vernal) Equinox

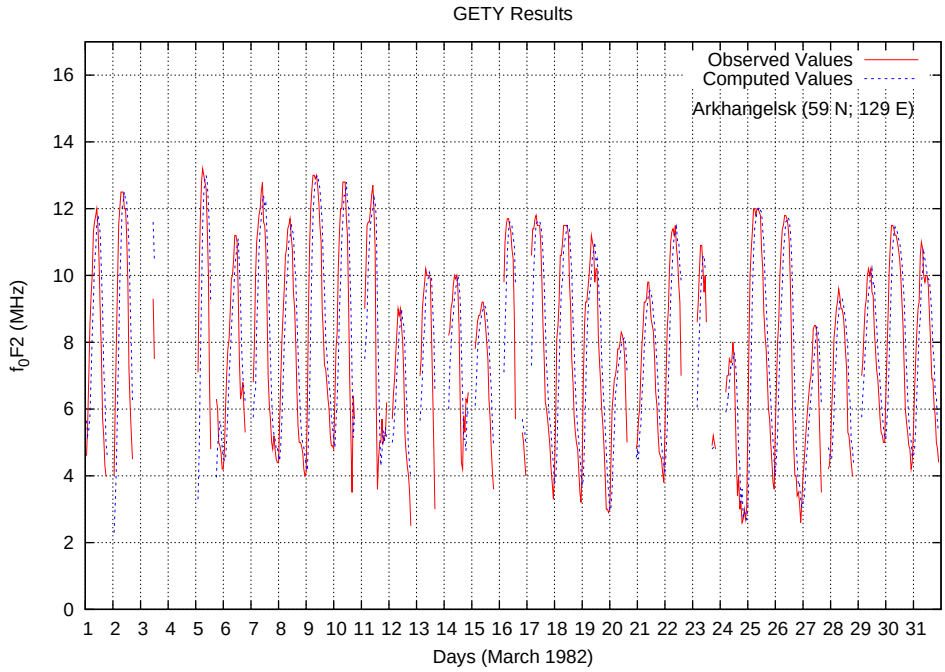

Figure 4.10: Observed Values (in red) and Genetic Programming Results (in blue) of f_0F2 values for March 1982 (around Spring Equinox)

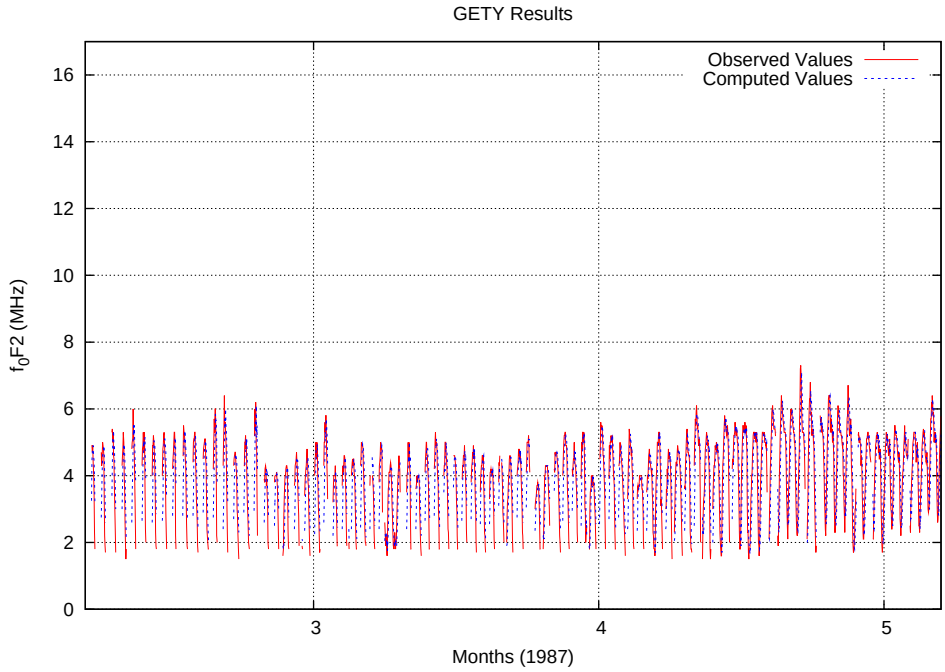

Figure 4.11: Observed Values (in red) and Genetic Programming Results (in blue) of f_0F2 values for the year 1987 around Spring (Vernal) Equinox

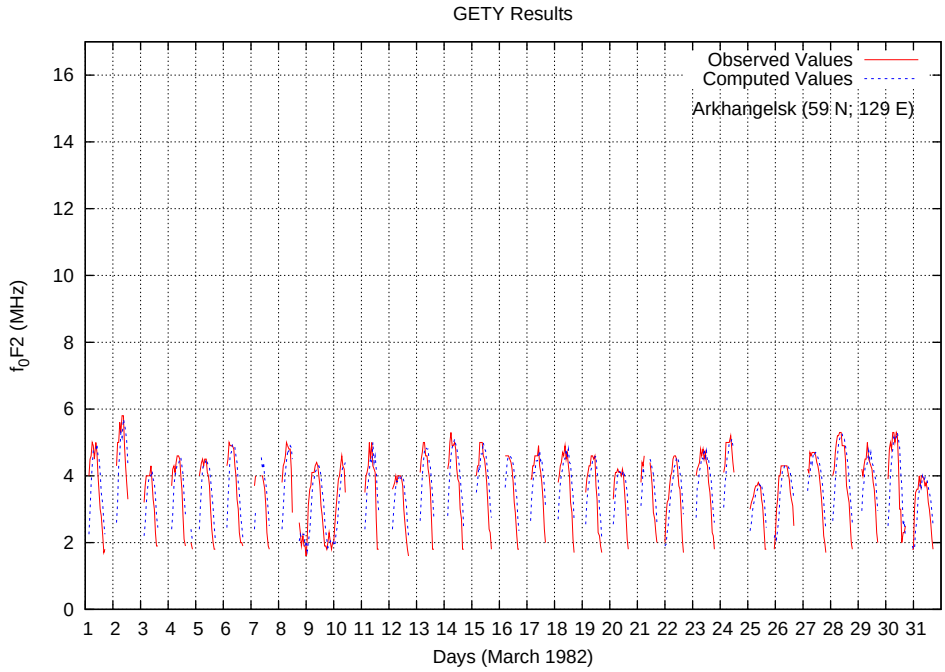

Figure 4.12: Observed Values (in red) and Genetic Programming Results (in blue) of f_0F2 values for March 1987 (around Spring Equinox)

The success of the combined model can be seen easily in Figures 4.13, 4.14, 4.15, 4.16 which were plots showing the computed and observed values of f_0F2 during Summer Solstice. The success of the model was high during summer, since the continuous data of f_0F2 during summer and lack of data of f_0F2 during winter impose to GP to create models having behaviours of summer. However, if more data was supplied to the model, then it would have been more successful for the whole year. The performance of the model, GETY-IYON, during Fall and Winter was also as high as performance during summer, but not higher than the performance of summer. The results of fall and winter were shown in Figures 4.17, 4.18, 4.19, 4.20, 4.21, 4.22.

The results plotted monthly showed that the model, GETY-IYON could also be used filling the data gaps.

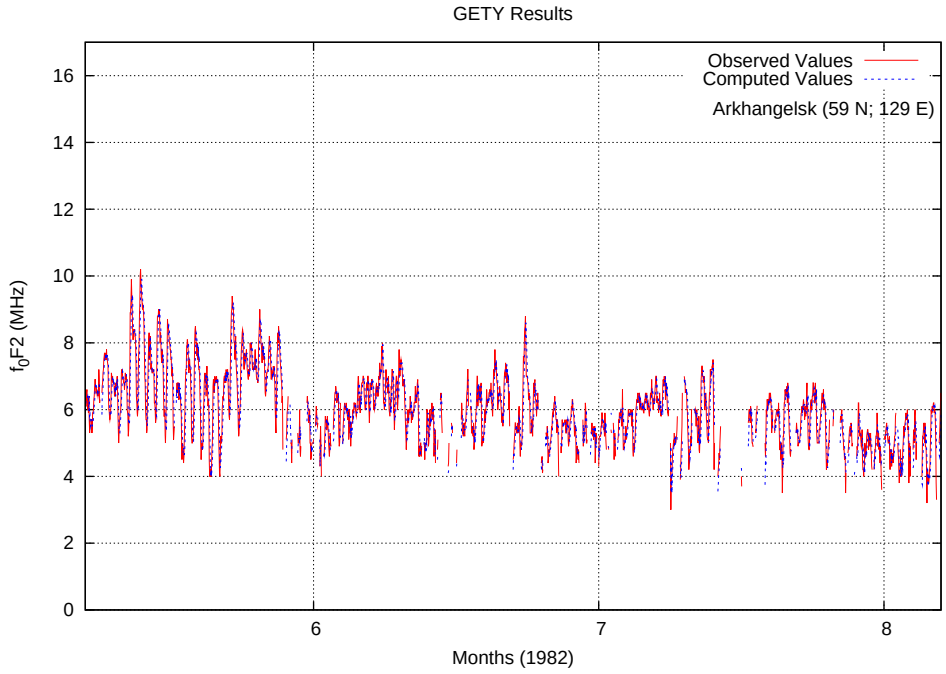

Figure 4.13: Observed Values (in red) and Genetic Programming Results (in blue) of f_0F2 values for the year 1982 around Summer Solstice

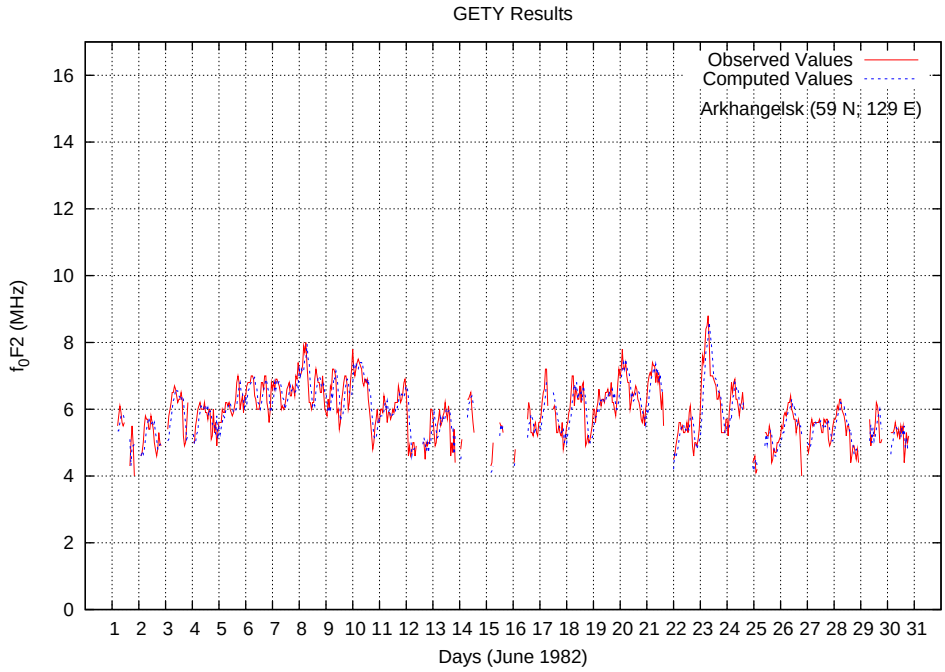

Figure 4.14: Observed Values (in red) and Genetic Programming Results (in blue) of f_0F2 values for June 1982 (around Summer Solstice)

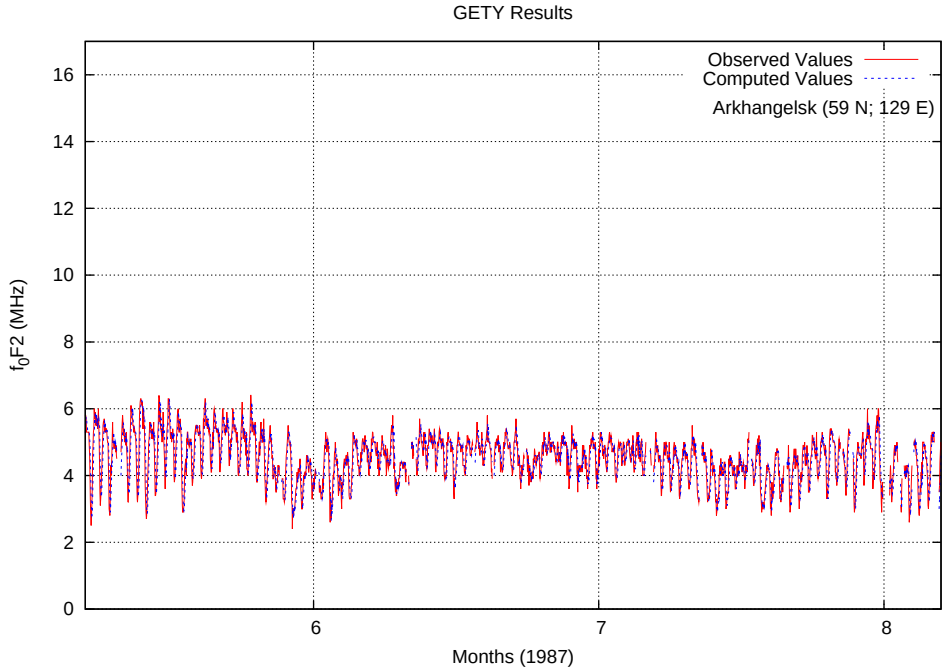

Figure 4.15: Observed Values (in red) and Genetic Programming Results (in blue) of f_0F2 values for the year 1987 around Summer Solstice

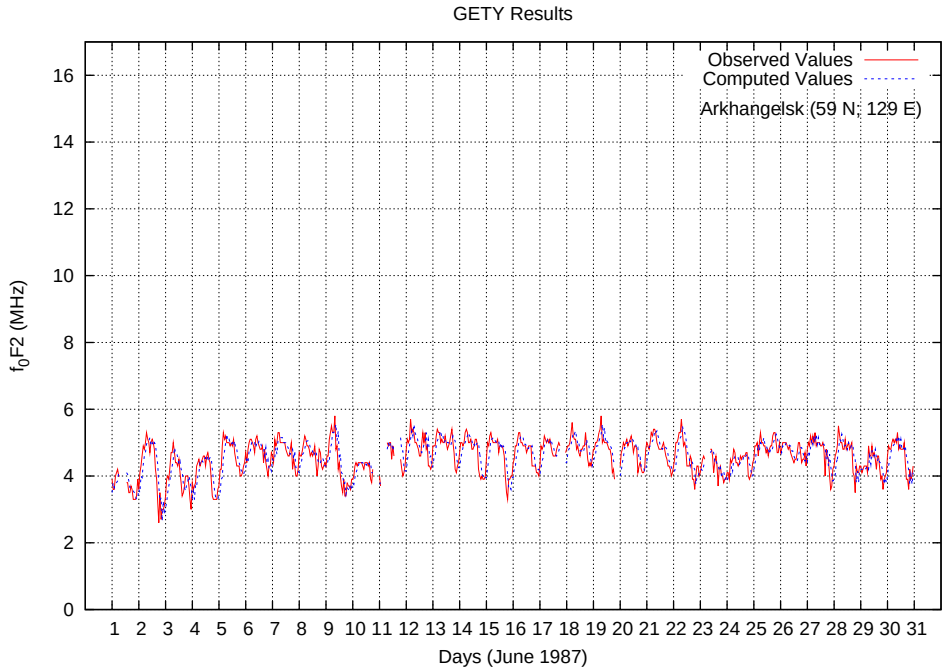

Figure 4.16: Observed Values (in red) and Genetic Programming Results (in blue) of f_0F2 values for June 1987 (around Summer Solstice)

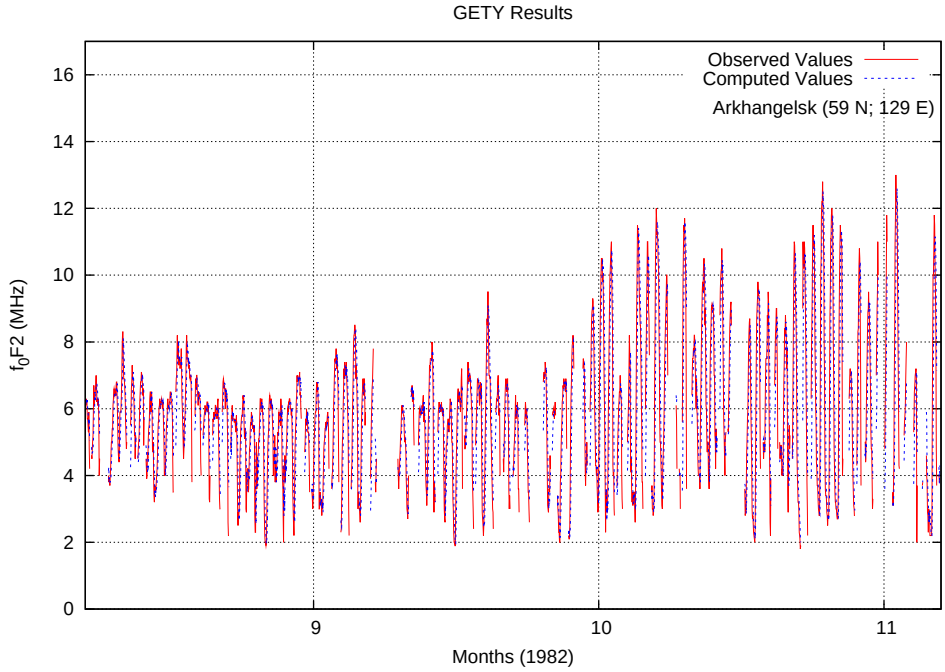

Figure 4.17: Observed Values (in red) and Genetic Programming Results (in blue) of f_0F2 values for the year 1982 around Fall (Autumnal) Equinox

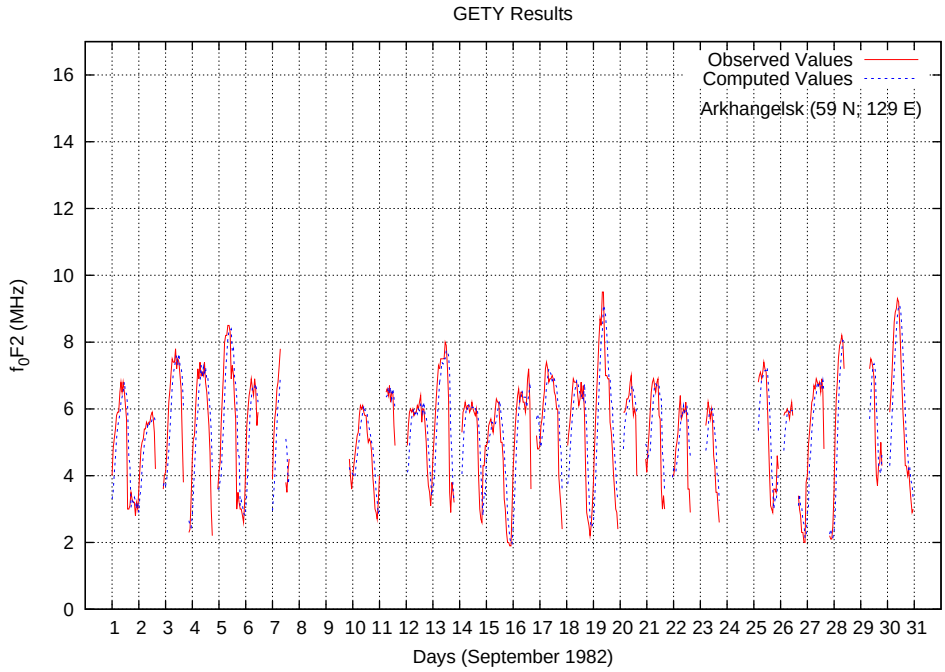

Figure 4.18: Observed Values (in red) and Genetic Programming Results (in blue) of f_0F2 values for September 1982 (around Fall (Autumnal) Equinox)

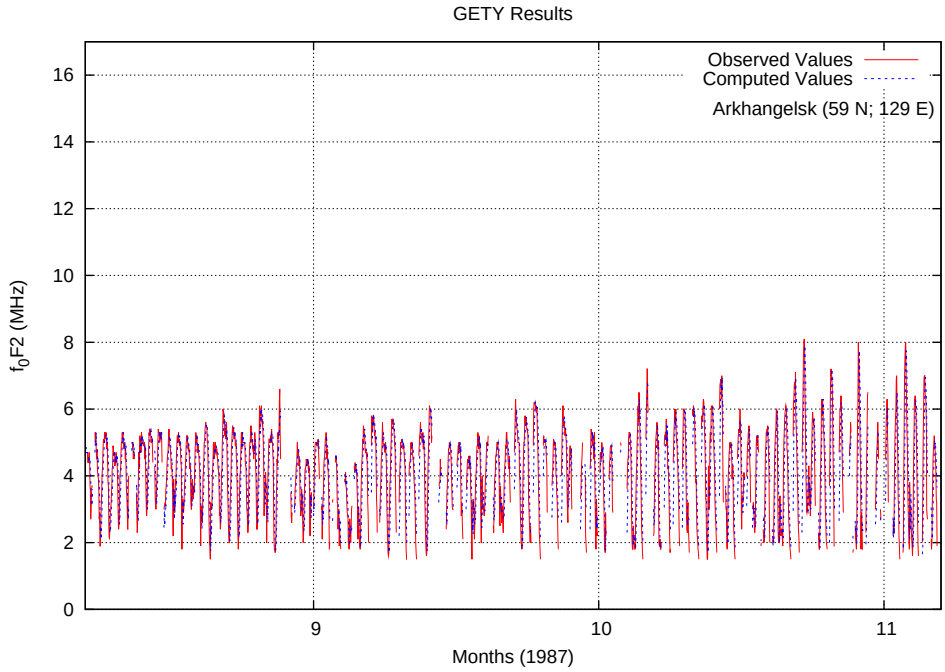

Figure 4.19: Observed Values (in red) and Genetic Programming Results (in blue) of f_0F2 values for the year 1987 around Fall (Autumnal) Equinox

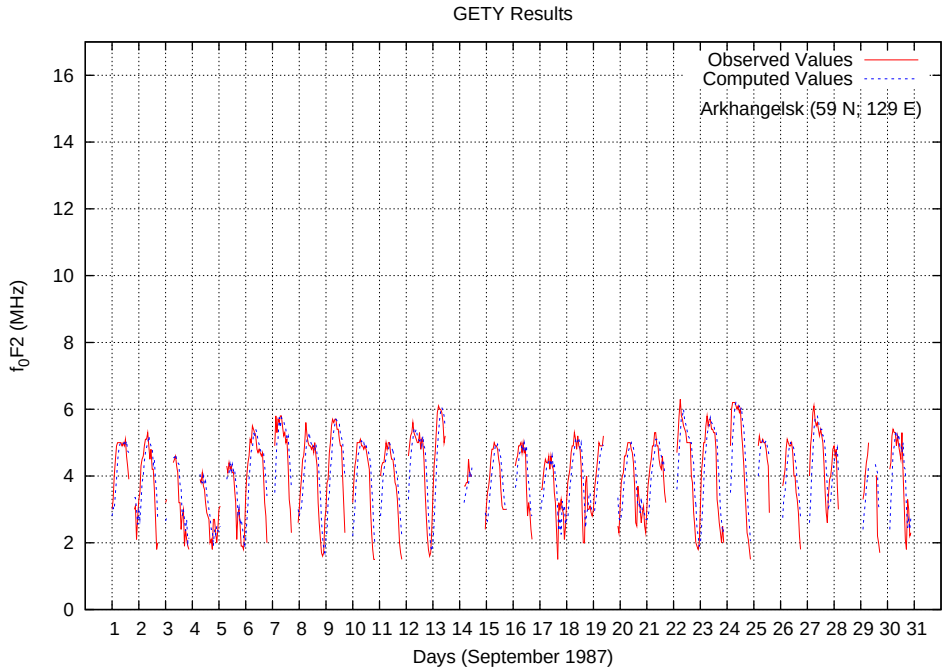

Figure 4.20: Observed Values (in red) and Genetic Programming Results (in blue) of f_0F2 values for September 1987 (around Fall (Autumnal) Equinox)

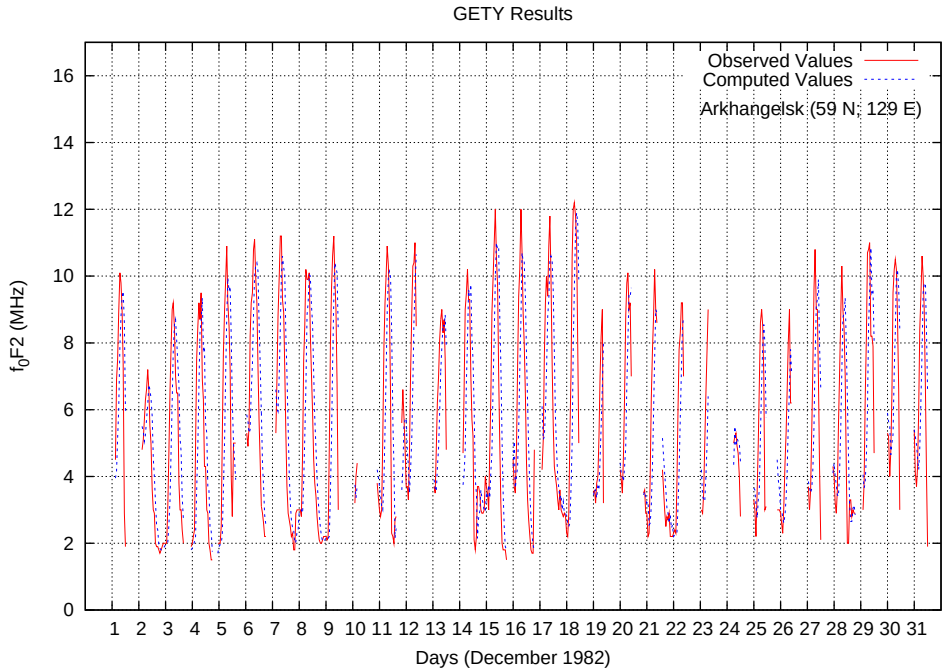

Figure 4.21: Observed Values (in red) and Genetic Programming Results (in blue) of f_0F2 values for December 1982 (around Winter Solstice)

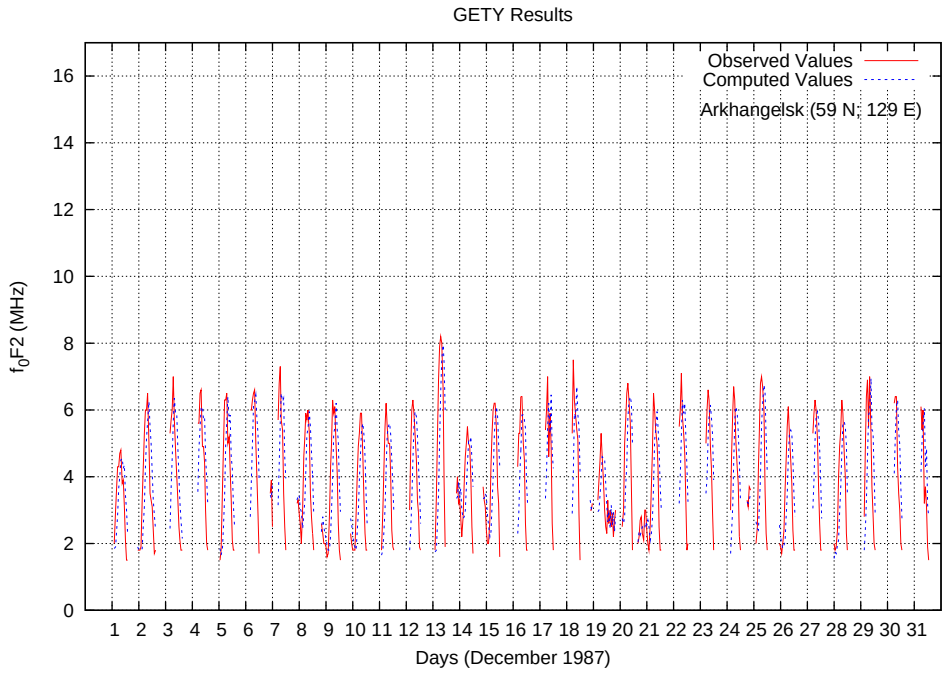

Figure 4.22: Observed Values (in red) and Genetic Programming Results (in blue) of f_0F2 values for December 1987 (around Winter Solstice)

CHAPTER 5

DISCUSSION and CONCLUSION

In this work, the influences of Interplanetary Magnetic Field has been investigated.

At the very beginning of the study, a simple statistical technique, Superposed Epoch Method, was employed. The results of the SPE has shown that there is a certain influence of Interplanetary Magnetic Field on the variability of Ionospheric F layer critical frequency, A polarity reversal in IMF B_z of magnitude 11nT/h resulted in a ~1 MHz decrease in the f_0F2 values. Also the effect of Interplanetary Magnetic Field on the variability of geomagnetic activity has been shown. The minimum Dst during the IMF B_z polarity reversals was computed to be about 60nT and the increase in the Kp values was calculated to be around 5. In addition, it has been seen that the quasi-steady IMF B_y polarity, increase the duration of the influence on geomagnetic activity.

Although the dependence of the geomagnetic activity on the IMF B_y could be observed, the influence of IMF B_y could not be shown in the f_0F2 values due to lack of data. Thus, in order to quantify the effect, another technique, Genetic Programming was employed. Using this technique, a model, GETY-IYON, which forecasts 1 hour ahead forecast of Ionospheric F layer critical frequency, was constructed. The overall error of the model was 7.3%. The success of the model was seen to be higher during summer, whereas the errors increased during winter. This difference was dependent on the dominance of the data during summer. It has been also concluded that the Genetic Programming was very effective in constructing a mathematical model in relation to a physical process, however it was very difficult to construct a model in forecasting a physical process.

REFERENCES

[1] Pulkkinen, P. Space Weather: Terrestrial Perspective, Living Rev. Solar Phys., 4, 2007

[2] Hartmann, D. L., ATM 552 Notes: Compositing, pages 32-34, 2007

[3] Cumnock, J. A., 2005. High-latitude aurora during steady northward interplanetary magnetic field and changing IMF B_y, J. Geophys. Res., 110, A02304, doi:10.1029/2004JA010867.

[4] Maynard, N. C., 2005. Couplng The Solar-Wind/IMF To The Ionosphere Through The High Latitude Cusps, Surveys in Geophysics, 26, 255-280.

[5] Reshetnyks, V.M. , 2005. Behaviour of auroral activity as a function of the interplanetary magnetic field, Planetary and Space Science, 53, 181-187.

[6] Wing S., P. T. Newell and C.I. Meng, 2005. Cusp Modeling and Observations at Low Altitude, Surveys in Geophysics, 26, 341-367

[7] Goodman, J. M., Space Weather&Telecommunications, Springer, 1st edition, 2004

[8] Prölls, G. W., Physics of the Earth's Space Environment, Springer, 2004

[9] Kallenrode, M. Space physics : an introduction to plasmas and particles in the heliosphere and magnetospheres (3rd ed.), Berlin: Springer, 2004

[10] Tulunay, Y., and Bradley, P., 2003. WP 1.1 Impact of Space Weather on Communication, COST 271 Technical Document, (TD 02 003)

[11] Russell, C.T., Fleishman, M., 2002. Joint control of region-2 field-aligned currents by the east-west component of the interplanetary electric field and polar cap illumination, Journal of Atmospheric and Solar-Terrestrial Physics, 64, 1803-1808.

[12] Aravindan, P., and Iyer, K. N., 2001. Day-to-day variability in ionospheric electron content at low latitudes, Planet. Space Sci., 38, 743-750.

[13] Bae, S.H., Lee, D.-Y., Lee, E., Min, K.W. , Choi, K.H., 2001. Substorms associated with azimuthal turnings of the interplanetary magnetic field, Journal of Atmospheric and Solar-Terrestrial Physics, 63, 1763-1774.

[14] Gombosi T., Physics of the Space Environment, Cambridge University Press, Cambridge, UK, 1998.

[15] Liou, K., Newell, P.T., Meng, C.-I., Brittnacher, M., Parks, G., 1998. Characteristics of solar wind controlled auroral emissions, J. Geophys. Res. 103, 17543

[16] Davis, J. D., Wild, M. N., Lockwood, M., Tulunay, Y., 1997. Ionospheric and geomagnetic responses to changes in IMF B_z: a superposed epovch study, Annal. Geophysicae, 15, 217-230.

[17] Tulunay, Y., 1996. Interplanetary magnetic field and its possible effects on the mid-latitude ionosphere III, Annali di Geofisica, 39/4, 853-862.

[18] Lyons, L.R., 1995, A new theory for magnetospheric substorms. J. Geophys. Res. A100, 19, 069

[19] Hapgood, M. A., Lockwood, M., Bowe , G. A., Willis, D. M., Tulunay, Y. K., 1994. Variability of the interplanetary medium at 1 a.u. over 24 years: 1963-1986, Planet. Space Sci., 39 (3), 411-423.

[20] Kivelson, M. G., Russell, C. T, Introduction to Space Physics, 3^{rd} Edt, Cambridge University Press, 1995

[21] Tulunay, Y., 1994. Interplanetary magnetic field and its possible effects on the mid-latitude ionosphere II, Annali di Geofisica, 37/2, 193-200.

[22] Tulunay, Y., 1994 Predictability of ionospheric variations for quiet and disturbed conditions, J. Atmos. Terr. Phys., 57, 1469-1481

[23] Koza, J.R., Genetic Programming, MIT Press, London, 1992.

[24] Bradley, P. A., 1991. Improvemets in the propagation prediction method to be used for HF broadcasting, ITU Telecommun. J., 58 (9), 558.

[25] McPherron, R.J., Terasawa, T., Nishida, A., 1986. Solar wind triggering of substorm onset, Journal of Geomagnetism and Geoelectricity, 38, 1089

[26] Nishida A., Geomagnetic Diagnosis of the Magnetosphere, Springer-Verlag, New York Heidelberg Berlin, 1978

[27] http://www.tp.umu.se/forskning/space/magnetosphere.jpg (Last retrieved on 30 April 2007)

[28] http://nssdc.gsfc.nasa.gov/space/imp-8.htm (Last retrieved on 3 June 2007)

[29] http://www.ngdc.noaa.gov/stp/GEOMAG/kp_ap.shtml (Last retrieved on 4 June 2007)

[30] http://www.gfz-potsdam.de/pb2/pb23/niemegk/kp_index/ (Last retrieved on 4 June 2007)

[31] http://www.spenvis.oma.be/spenvis/help/background/coortran/coortran.html#ILL (Last retrieved on 14 June 2007)

APPENDIX A

Coordinate Systems

A.1 The Geocentric Solar Ecliptic System

"The Geocentric Solar Ecliptic System (GSE) has its X-axis pointing from the Earth towards the sun and its Y-axis is chosen to be in the ecliptic plane pointing towards dusk (thus opposing planetary motion). Its Z-axis is parallel to the ecliptic pole. Relative to an inertial system this system has a yearly rotation."[31]

A.2 Geocentric Solar Magnetospheric System

"The Geocentric Solar Magnetospheric System (GSM), as with both the GSE system, has its X-axis from the Earth to the Sun. The Y-axis is defined to be perpendicular to the Earth's magnetic dipole so that the X-Z plane contains the dipole axis. The positive Z-axis is chosen to be in the same sense as the northern magnetic pole. The difference between the GSM system and the GSE and GSEQ is simply a rotation about the X-axis."[31]

APPENDIX B

Relevant Publications and Activities

Publications

- International Publications

1. T. Yapıcı, Y. Tulunay, 2007. Possible Influences of Interplanetary Magnetic Field on the Ionospheric Variability: A modeling approach, Advances in Space Research (submitted)
2. Y. Tulunay, E. Tulunay, E. Altuntaş, T. Yapıcı, Near Earth Space Activities: A Turkish Initiative - IHY 2, Sun and Geosphere, 1, 2006

- National Publications

None

Activities

- International Conferences

1. Modeling Ionospheric and Solar Parameters using Genetic Programming Approach, IRI/COST 296 Workshop: Ionosphere - Modelling, Forcing and Telecommunications, 10-14 July, 2007, Prague, Czech Republic, Y. Tulunay, T. Yapıcı, E. Tulunay, Z. Kocabaş
2. Further Investigation of the Possible Effects of the IMF B_z and IMF B_y components on the Ionospheric f_0F2 values, Third European Space Weather Week, 13-17 November 2006, Brussels, Belgium, Y. Tulunay, T. Yapıcı, E. Tulunay
3. A New Integrated European Space Weather Portal, Third European Space Weather Week, 13- 17 November 2006, Brussels, Belgium, K. Stegen, J. Lilensten, A. Glover, A. Hilgers, D. Heynderickx, J. Wera, M. Messerotti, I. Stanislavska, T. Yapıcı, P. Gilles
4. The Probable Effects of Interplanetary Magnetic Field (on the F-layer Critical Frequency), International Symposium on Recent Observations and Simulations of the Sun-Earth System (ISROSES), 17-22 September 2006, Varna, Bulgaria, T. Yapıcı, Y. Tulunay
5. Propagation Related Measurements During Three Solar Eclipses in Turkey, 10^{th} International Conference on Ionospheric Radio Systems & Techniques, 18-21 July 2006, London, E. Tulunay, E. M. Warrington, Y. Tulunay, Y. Bahadırlar, A. S. Türk, R. Çaputçu, T. Yapıcı, E. T. Şenalp

6. COST296 WG2.2 Activity Report : Radio Propagation Measurements During the 29 March 2006 Total Eclipse Week, 4^{th} COST 296 MCM and WG meetings, 27-29 April 2006, Neustrelitz, Germany, E. Tulunay, M. Warrington, Y. Tulunay, Y. Bahadırlar, A. S. Türk, T. Yapıcı, E. T. Şenalp, E. Altuntaş, Ö. Sarı, O. Büyükpapuşcu
7. The effects of IMF B_z on the F-layer Critical Frequency, 8^{th} COST 724 MCM and WG meetings, 27-30 March 2006, Antalya, Turkey, Y. Tulunay, T. Yapıcı
8. Neural Network Modeling in Forecasting the Near Earth Space Parameters: the Near Earth Space Parameters: Forecasting of the Solar Radio Fluxes Forecasting of the Solar Radio Fluxes, COST 724 MCM, 10-13 Oct. 2005, Athens, Y. Tulunay, M. Messerotti, E. T. Şenalp, E. Tulunay, M. Molinaro, Y. I. Özkök, T. Yapıcı, E. Altuntaş, N. Çavuş

- National Conferences

1. Gezegenlerarası Manyetik Alanın Kritik Frekans Üzerine Etkisi, I. Ulusal Havacılık ve Uzay Konferansı, 21-23 September 2006, METU, Ankara, Turkey, T. Yapıcı, Y. Tulunay
2. Gezegenlerarası Manyetik Alan ve Yer'e Yakın Uzay'daki Olası Etkileri, Kayseri VI. Havacılık Sempozyumu, 12-14 May 2006, Nevşehir, Turkey, Yurdanur Tulunay, Tolga Yapıcı

- Projects and Short Term Scientific Missions

1. EU COST 724 (Developing the Scientific Basis for Monitoring, Modeling and Predicting Space Weather), Researcher, 2005-
2. EU COST 724 (Developing the Scientific Basis for Monitoring, Modeling and Predicting Space Weather) - International Heliophysical Year (IHY), "I LOVE MY SUN" Outreach Activity
3. EU COST 724 Short Term Scientific Mission (STSM), Warsaw, Poland, 18-23 June 2006
   - Implementing METU-NN model through COST 724 Web Server
   - Help implementing any other models/databases to current Web Server
   - Attend probable Work Bench at the Polish Academy of Science Space Research Centre if such need arises